Recruitment of Histone Methyltransferase Ehmt1 to Foxp3 TSDR Counteracts Differentiation of Induced Regulatory T Cells

Martin Karl [1], Christian Sommer [2], Christian H. Gabriel [1], Katharina Hecklau [1], Melanie Venzke [1], Anna Floriane Hennig [1], Andreas Radbruch [3,4], Matthias Selbach [2] and Ria Baumgrass [1]

1 - Signal Transduction, *German Rheumatism Research Center (DRFZ), A Leibniz Institute, Charitéplatz 1, 10117 Berlin, Germany*
2 - Proteome Dynamics, *Max Delbrück Center for Molecular Medicine in the Helmholtz Association, Robert-Rössle-Str. 10, 13125 Berlin, Germany*
3 - Cell Biology, *German Rheumatism Research Center (DRFZ), A Leibniz Institute, Charitéplatz 1, 10117 Berlin, Germany*
4 - Charité—University Medicine, *Charitéplatz 1, 10117 Berlin, Germany*

Correspondence to Ria Baumgrass: *Deutsches Rheuma-Forschungszentrum Berlin, Charitéplatz 1, D-10117 Berlin, Germany.* baumgrass@drfz.de
https://doi.org/10.1016/j.jmb.2019.07.031

Abstract

Differentiation toward $CD4^+$ regulatory T (Treg) cells is essentially dependent on an epigenetic program at Treg signature genes, which involves remodeling of the Treg-specific demethylated regions (TSDRs). In particular, the epigenetic status of the conserved non-coding sequence 2 of Foxp3 (Foxp3 TSDR) determines expression stability of the master transcription factor and thus Treg lineage identity. However, the molecular mechanisms controlling the epigenetic remodeling at TSDRs in Treg and conventional T cells are largely unknown.

Using a combined approach of DNA pull-down and mass spectrometric analysis, we report a novel regulatory mechanism in which transcription factor Wiz recruits the histone methyltransferase Ehmt1 to Foxp3 TSDR. We show that both Wiz and Ehmt1 are crucial for shaping the region with the repressive histone modification H3K9me2 in conventional T cells. Consistently, knocking out either Ehmt1 or Wiz by CRISPR/Cas resulted in the loss of H3K9me2 and enhanced Foxp3 expression during iTreg differentiation. Moreover, the essential role of the Wiz–Ehmt1 interaction as observed at several TSDRs indicates a global function of Ehmt1 in the Treg differentiation program.

Introduction

Tolerance toward self and innocuous foreign antigens is crucial for immunological homeostasis. Among the $CD4^+$ T cell populations with regulatory functions, a subset characterized by the expression of the master transcription factor *forkhead box P3* (Foxp3; further referred to as Treg cells) plays a central role in tolerance by suppression of misdirected immune reactions of effector T-cell subsets. Treg cells comprise about 10% of the $CD4^+$ T-cell pool and are mainly generated during a selection process in the thymus (thymus-derived Treg, or tTreg) due to autoantigen specificity [1]. Alternatively, Treg cells differentiate from naïve $CD4^+$ T cells in the periphery to ensure tolerance toward foreign antigens (peripheral induced Treg, or pTreg). pTreg differentiation is regulated *via* TGF-β [2]. Accordingly, Foxp3 expression and other Treg-specific characteristics can be induced during culture of naïve cells in the presence of TGF-β *in vitro* [3]. These *in vitro* induced Treg (iTreg) cells have been widely used as models to study Treg differentiation. However, iTreg cells do not completely recapitulate the full Treg phenotype of naturally occurring Treg cells (nTreg; i.e., the entirety of tTreg and pTreg cells) in terms of epigenetic remodeling and an unstable expression pattern of nTreg signature genes [1,4,5].

The Treg differentiation program is guided by distinct axes of regulation, such as (i) a network of five core transcription factors that robustly lock in the program, (ii) expression control by the master transcription factor Foxp3, and (iii) Foxp3-independent epigenetic remodeling at regulatory regions of signature genes involving DNA hypomethylation (i.e., Treg-specific demethylated regions; TSDRs) [4,6–10]. Strikingly, expression of Foxp3 itself is tightly regulated by all three mechanisms [7,10–13].

Stable and heritable expression of Foxp3 is an essential prerequisite for Treg differentiation and suppressive function and thus is crucial for balanced immune responses and immunological tolerance. In addition to its promoter, the Foxp3 locus comprises three highly *conserved non-coding sequences* (CNS; Fig. 1a). These fulfill distinct module-like functions in the expression control of Foxp3 acting as a pioneer element for the expression initiation (CNS3), as a TGF-β sensor during pTreg (and iTreg) differentiation (CNS1), and as a regulator of the maintenance of expression in homeostasis and in inflammatory environments (CNS2), respectively [4,5,11,17–20].

CNS2 harbors a CpG-enriched element that is epigenetically regulated by differential DNA methylation, which is also referred to as Foxp3 TSDR [4]. This region is hypermethylated in naïve and conventional T (Tcon) cells. Only in Treg cells is complete demethylation actively catalyzed by methylcytosine dioxygenases of the *ten–eleven translocation* (Tet) family [13,20–22]. This mechanism appears to be guided by IL-2 and is implemented with stage-dependent kinetics during tTreg differentiation [21,22]. Of the 14 CpG residues within the region, CpGs 9, 12, 13, and 14 are demethylated early and are located in the downstream half of the region indicating an initiation function for the epigenetic opening of the TSDR within this part [22] (Fig. 1a). Hypomethylation of the TSDR allows for the binding of activating transcription factors, among them *v-ets erythroblastosis virus E26 oncogene homolog 1* (Ets1), *cAMP-responsive element binding protein 1* (Creb1)/*activating transcription factor 1* (Atf1), and Foxp3 itself [11,14,15]. Most importantly, the hypomethylated status is mandatory for stable Foxp3 expression and therefore Treg lineage identity, especially in a pro-inflammatory environment [5,23,24].

The significance of the epigenetic remodeling at the Foxp3 TSDR is reflected most clearly during iTreg differentiation. Here, DNA demethylation remains incomplete, correlating with the loss of Foxp3 expression after restimulation [5]. Most recently, supplementation of differentiation cultures with vitamin C has been found to mediate DNA demethylation and, correspondingly, stable Foxp3 expression in iTreg cells, even in a transfer model of alloantigen-induced iTreg cells [22,25,26]. This effect of vitamin C was dependent on Tet enzyme activity and appears to be Treg specific, since cells cultured under Th0 conditions maintained the hypermethylated status [22,25]. However, the underlying mechanisms guiding the remodeling of the Foxp3 TSDR are largely unknown, and other levels of epigenetic modifications have not yet been rigorously addressed. In addition, signals and kinetics that drive Treg-specific epigenetic remodeling at other TSDRs are far from being completely understood. Indeed, previous reports presented partially conflicting data about the role of vitamin C on DNA demethylation at these regions [22,25].

Euchromatic histone-lysine N-methyltransferase 1 (Ehmt1; also GLP, Kmt1b) and Ehmt2 (also G9a, Kmt1c) play important roles in the epigenetic control at euchromatin. They preferentially heterodimerize, thereby forming the key methyltransferase to catalyze mono- and dimethylation of lysine 9 at histone 3 (H3K9me1/me2) [27–30]. In the course of differentiation programs, Ehmt1/2 have been shown to regulate alternative splicing, transcriptional termination, the establishment of proviral silencing and facultative heterochromatinization *via* selective deposition of epigenetically repressive H3K9me2 at target sites [31–35]. In addition, an interaction of the Ehmt enzyme complex with DNA methyltransferases Dnmt1, Dnmt3a, and Dnmt3b, and thus an interconnection of DNA methylation and H3K9 methylation, has been demonstrated at several shared target sites in embryonic stem (ES) cells [36–38]. In detail, Ehmt2 deficiency resulted in alterations of the DNA methylation pattern as well as promiscuous gene expression during imprinting of ES cells and embryonic development, thereby highlighting an essential role of Ehmt enzymes within these epigenetic programs [36,39–42].

Here, we reveal differential H3K9me2 deposition as a determining level of epigenetic regulation at the Foxp3 TSDR and characterize the underlying molecular mechanism. Using an unbiased DNA pull-down approach, we identified transcription factor Wiz to be crucial for the recruitment of the Ehmt enzyme complex to maintain H3K9me2 at Foxp3 TSDR in Tcon cells as well as iTreg cells cultured without vitamin C. We further demonstrate co-regulation of H3K9me2 and DNA methylation at the Foxp3 TSDR during Treg differentiation and discuss that these epigenetic marks cooperate to create a repressive epigenetic landscape at the region. Remarkably, the observed dependency of H3K9me2 at the Foxp3 TSDR and other TSDRs on the action of Wiz and Ehmt1, but less significant on Ehmt2, suggests a specialized role for Ehmt1 in the Treg differentiation program.

Results

Histone methyltransferases Ehmt1/Ehmt2 are recruited to a sequence of Foxp3 TSDR

Epigenetic remodeling at the Foxp3 TSDR is of particular importance for the stability of Foxp3 expression in Treg cells [5,23,24]. To discover epigenetic modulators, we used an unbiased strategy for identifying so far unknown protein–DNA interactions at the TSDR by application of DNA pull-down with mass spectrometric analysis (PD-MS) [43]. PD-MS experiments were restricted to an oligo sequence length of 40 bp to allow for comparative analysis with reliable scrambled control sequences. We focused on a functional element of the murine Foxp3 TSDR, which harbors CpGs 10–12 as well as

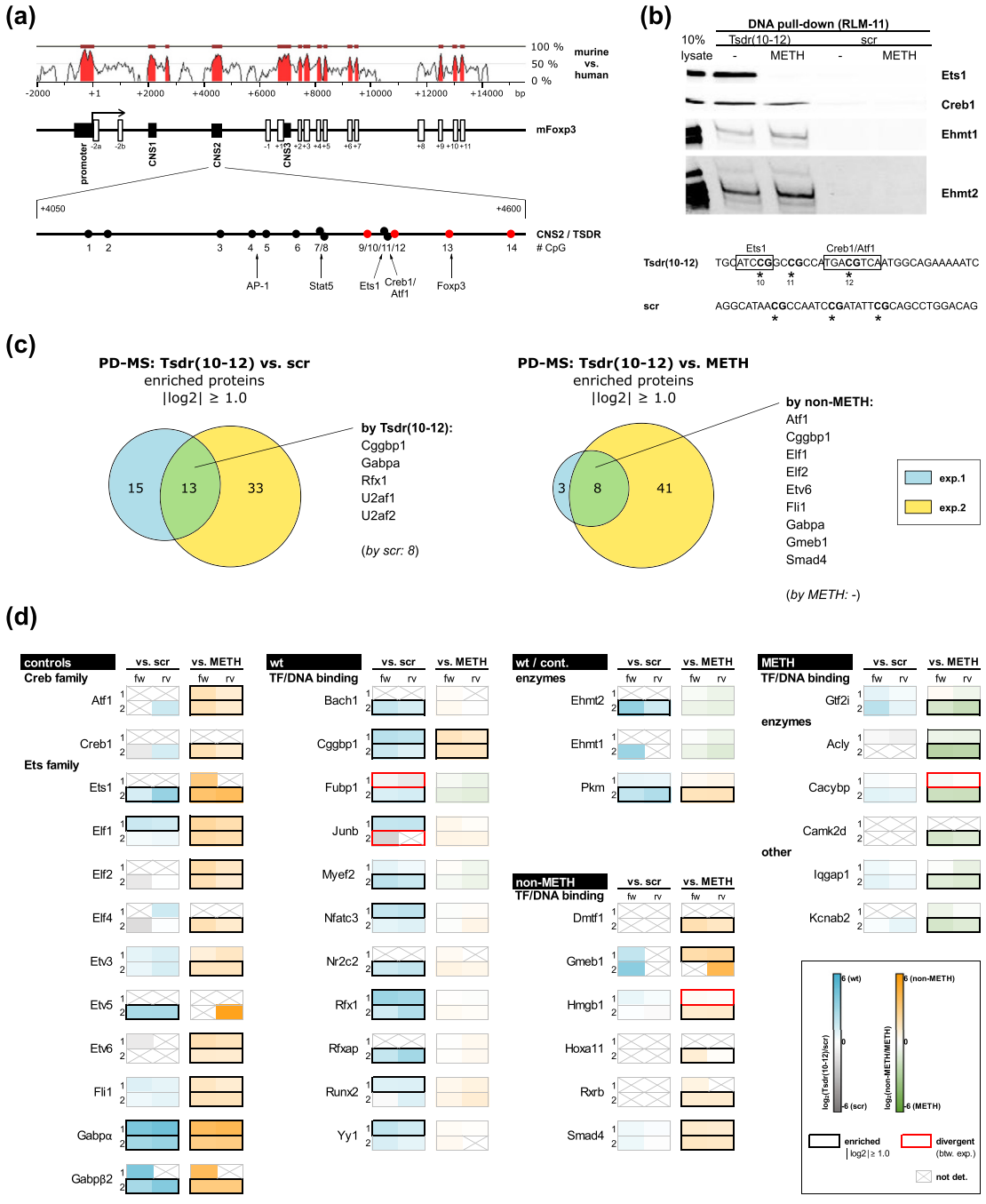

Fig.1 (*legend on next page*)

binding sites for Ets1 and Creb1/Atf1 and which is located within that half of the region exhibiting early DNA demethylation during tTreg cell differentiation [14,15] (Fig. 1a and b). First, classical DNA pull-down followed by Western blot (PD-WB) with the respective 37-bp oligonucleotide Tsdr(10−12) and nuclear extracts from the murine $CD4^+$ $CD8^-$ lymphoma cell line RLM-11 confirmed sequence-specific and methylation-sensitive binding of both Ets1 and Creb1 [14,15] (Fig. 1b).

Subsequently, *stable isotope labeling by amino acids in cell culture* (SILAC) [44] and DNA pull-down combined with mass spectrometric analysis (Supplementary Fig. S1a; see Supplementary Information for details) allowed to screen for so far unknown DNA-protein interactions at Tsdr(10−12). In detail, we compared DNA pull-down eluates from oligo Tsdr(10−12) to a scrambled (scr) control as well as from the non-methylated to the methylated (METH) oligo Tsdr(10−12) in two independent experiments (biological replicates; Supplementary Fig. S2; Supplementary Table S1a). Roughly 450−700 proteins were identified in the individual comparisons with overall consistency between the forward and reverse experiments (Pearson correlation coefficient r ranging from −0.51 to −0.75; Supplementary Table S1b). Of these, 2−17 proteins were enriched ($|\log_2(H/L)| \geq 1.0$ for both fw and rv samples) by one condition in experiment 1 and twice this number in experiment 2 (16−30 hits; Supplementary Table S1d, e, h, i; Fig. 1c). The second experiment reproduced 46% or 73% of hits identified in the first experiment, respectively (Fig. 1c). Furthermore, proteins that were identified in both experiments showed overall consistent enrichment ratios (Fig. 1d, Supplementary Fig. S3a).

When detected adequately, the known interactors Ets1, Creb1, and Atf1 were enriched specifically for the non-methylated sequence in comparison to the methylated oligonucleotide Tsdr(10−12) (*versus* METH) and for Ets1 also in comparison to the scrambled control (*versus* scr; Fig. 1d). We have to note that for Creb1, one particular data point within the comparison to scrambled was divergent between the respective forward and reverse experiment. In agreement with the high conservation of the Ets family binding motif [45], other Ets family members exhibited a behavior similar to Ets1 (Fig. 1d). Moreover, several other transcription factors and putative co-factors were enriched by Tsdr(10−12) in the PD-MS screen (Fig. 1d; Supplementary Fig. S2). With the exception of the particular divergent Creb1 data point, subsequent investigation using classical PD-WB consistently validated the PD-MS data of all proteins tested (Supplementary Fig. S3b).

However, epigenetic modifiers and readers, such as Dnmt proteins, typical DNA methylation binders, histone modifying enzymes, and Tet proteins were hardly detected or showed no specific enrichment by Tsdr(10−12) (Supplementary Fig. S1b). Only histone methyltransferase Ehmt2 was enriched compared to the scr control in the PD-MS screen (Fig. 1d). In addition, both Ehmt2 and its interaction partner Ehmt1 exhibited moderate preference for the methylated state (Tcon characteristic; mean $|\log_2(\text{METH/non-METH})| = 0.55$ and 0.61, respectively) (Fig. 1b, d). In *ex vivo* isolated "resting" naïve and nTreg cells, Ehmt1 and Ehmt2 protein levels were found to be low but increased massively after 2−3 days of *in vitro* culture (not on RNA level; Supplementary Fig. S5a, b). Consistently, DNA pull-down with nuclear extracts from activated $CD4^+$ T

Fig. 1. Ehmt1/Ehmt2 are recruited to oligo Tsdr(10−12) in DNA pull-down. (a) The murine Foxp3 locus harbors four conserved non-coding sequences (CNS) exhibiting regulatory functions in gene expression control (promoter and CNS1−3; black boxes, top). CNS2, also referred to as Treg-specific demethylated region (TSDR), contains 14 CpG dinucleotides that are hypomethylated specifically in nTreg cells. Demethylation occurs first at CpGs 9, 11, 13, and 14 (thymic Treg differentiation; red dots, bottom). Transcription factors Creb1/Atf1, Ets1, Foxp3, and others have been shown to bind to Foxp3 TSDR in Treg cells [11,14−16]. Gene positions are given in bp relative to the transcriptional start site. (b) For DNA pull-down, a 37-bp sequence within murine Foxp3 TSDR was selected that harbors CpG dinucleotides 10−12 and binding sites for Ets1 and Creb1/Atf1 [Tsdr(10−12); bottom]. Sequences of Tsdr(10−12) and a scrambled control (scr) are shown in sense. Asterisks mark cytosine residues within CpG dinucleotides that were replaced by 5-methylcytosine in DNA-methylated variants of the oligonucleotides. DNA pull-down was performed with nuclear extracts of RLM-11 cells stimulated by PMA/ionomycin for 5 h (top). Eluates pulled down by oligonucleotide Tsdr(10−12), scr, or CpG methylated variants (METH, all oligos S1 nuclease-treated) were compared to 10% of input nuclear extract (lysate) by WB analysis. Data are representative of at least four independent experiments. (c and d) DNA pull-down experiments with subsequent mass spectrometric analysis (PD-MS) were performed with SILAC-labeled nuclear extracts of RLM-11 cells. Eluates of non-methylated oligo Tsdr(10−12) were compared to scrambled oligo (*versus* scr) or methylated Tsdr(10−12) (*versus* METH) in two independent experiments (biological replicates; exp. 1 and exp. 2). Enrichment of proteins was determined by the $\log_2$ of normalized SILAC ratios (heavy/light) of the forward (fw) and reverse (rv) samples. (c) Venn diagrams depict the overlap of enriched proteins ($|\log_2| \geq 1.0$ for both fw and rv samples) between experiments 1 and 2. (d) The heat map depicts proteins enriched in at least one comparison/experiment. Hits enriched by scr sequence or associated with single-strand binding were excluded. Hits were subdivided into categories (transcription factor, or TF). For better comparison, enrichment values were calculated by $\log_2$(non-methylated Tsdr(10−12)/other). Enrichment values of exps. 1 and 2 are depicted one below the other.

cells reproduced enrichment of Ehmt1 and Ehmt2 by oligo Tsdr(10−12) indicating sufficient conditions for Ehmt recruitment in primary T cells (not shown).

Enzymatic activity of Ehmt enzymes ensures H3K9me2 at Foxp3 TSDR in Tcon cells

Given the significant role of histone methyltransferases Ehmt1/Ehmt2 in ES cells [36,39,41,46−48], we investigated their role by determining H3K9me2 at regulatory regions of the Foxp3 locus in $CD4^+$ T cells. Chromatin immunoprecipitation (ChIP) demonstrated low levels of H3K9me2 at several Foxp3 regulatory regions in *ex vivo* isolated nTreg cells, which were maintained after *in vitro* culture (Fig. 2a; Supplementary Fig. S6a). In contrast, naïve $CD4^+$ T cells as well as *in vitro* differentiated Th1, Th2, and also iTreg cells possessed enriched H3K9me2, in particular at the TSDR indicating a role for Ehmt1/Ehmt2 in the epigenetic regulation of Foxp3 (Fig. 2a).

To prove Ehmt enzymatic activity at the Foxp3 TSDR, two selective inhibitors, UNC0638 [49] or BIX-01294 [50], were applied during *in vitro* differentiation. Indeed, both inhibitors led to a marked decrease of H3K9me2 levels especially at the TSDR and independent of subtype-skewing conditions resulting in a pattern which was comparable to nTreg cells (Fig. 2b, Supplementary Fig. S6b). However, BIX-01294 was excluded from further analyses due to considerable side effects on proliferation and cell survival.

To investigate whether H3K9me2 has a direct effect on other epigenetic marks at the Foxp3 TSDR, we determined H3K9 acetylation (H3K9ac) and DNA methylation at the region. However, the activating histone mark H3K9ac was low at the Foxp3 TSDR even in nTreg cells indicating no particular role for this mark in regulating the region's function (Supplementary Fig. S6c). Furthermore, MeDIP analysis and bisulfite sequencing revealed no differences of the DNA methylation status in UNC0638-treated and untreated iTreg cells, indicating that H3K9me2 itself is not necessary to maintain DNA methylation (Supplementary Fig. S6d, e). We cannot exclude that other H3K9 methyltransferases (e.g., Setdb1) may partially compensate for the inhibited enzymatic activity of Ehmt1/Ehmt2 by maintaining H3K9me1. However, to our knowledge, there are no hints for activity or recruitment of such enzymes to the Foxp3 TSDR.

Taken together, naïve cells, *in vitro* differentiated Tcon cells, and unstable iTreg cells possess high H3K9me2 levels at Foxp3 TSDR, which are maintained by the activity of Ehmt enzymes. Chemical inhibition of the histone methyltransferase activity, however, was not sufficient to stimulate the remodeling of the DNA methylation status in iTreg cells.

Vitamin C modulates the H3K9me2 status of Foxp3 TSDR during iTreg differentiation

Most recently, it has been demonstrated that vitamin C supplementation during iTreg differentiation is necessary and sufficient for complete DNA demethylation of the Foxp3 TSDR facilitating stable Foxp3 expression [25]. Therefore, we investigated the effect of vitamin C on H3K9me2. In line with a previous report [22], vitamin C increased (i) the percentage of $Foxp3^+$ cells and the Foxp3 protein amount on single cell level (Fig. 3a), (ii) iTreg-specific DNA demethylation of the TSDR (Supplementary Fig. S7b), and (iii) stability of Foxp3 expression in an *in vitro* stability assay (Supplementary Fig. S7c). Moreover, in accordance with DNA methylation remodeling, iTreg cells cultured in the presence of vitamin C also exhibited striking demethylation of H3K9me2 to a level similar to nTreg cells at the Foxp3 TSDR (Fig. 3b). Importantly, vitamin C treatment did not alter the expression of Ehmt1 or Ehmt2, nor were their protein levels affected (Supplementary Fig. S7d, e).

In contrast to iTreg cells, vitamin C did not affect H3K9me2 or DNA methylation at the Foxp3 TSDR during differentiation toward Th1 cells (Supplementary Fig. S7b and not shown). Therefore, we asked whether the H3K9 methylation is crucial for stable DNA methylation at the TSDR in Th1 cells. Application of the Ehmt inhibitor UNC0638 demonstrated that lack of H3K9me2 did not alter the hypermethylated DNA status of the Foxp3 TSDR, even not under adequate availability of vitamin C (Supplementary Fig. S7b).

Next, we studied whether demethylation of both epigenetic marks is functionally linked during iTreg cell differentiation. Several histone demethylases of the Jumonji C (JmjC)-domain-containing type have been described to actively erase H3K9me2 (such as Kdm3a and all members of Kdm4 [51]) and might be dependent on vitamin C [51,52]. Dimethyloxalylglycine (DMOG) is a competing substitute for 2-oxoglutarate (2OG) and inhibits the activity of JmjC histone demethylases as well as Tet enzymes [53,54] as both are members of the class of Fe(II) and 2OG-dependent dioxygenases. Strikingly, DMOG not only abrogated the beneficial effects of vitamin C on enhanced Foxp3 expression, but it also interfered with both demethylation of H3K9me2 at the Foxp3 TSDR as well as stability of Foxp3 expression (Fig. 3a, b; Supplementary Fig. S7c).

In summary, our results demonstrate vitamin C-dependent and iTreg-specific demethylation of H3K9me2 and DNA at the Foxp3 TSDR. DMOG-treatment abrogated the epigenetic remodeling and accordingly prevented iTreg cell stability indicating the importance of dioxygenases in establishing an epigenetic landscape that is a prerequisite for the stable Treg phenotype.

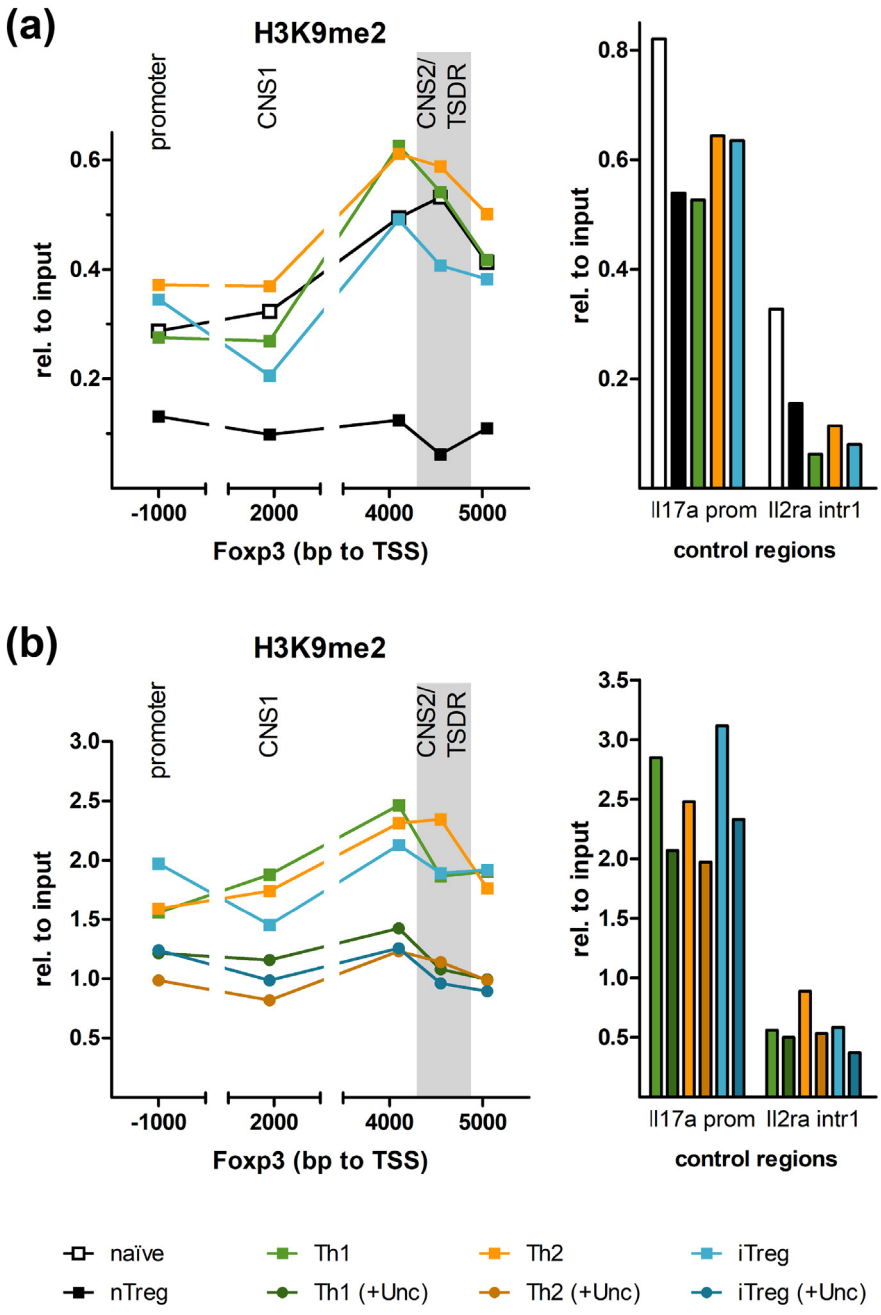

Fig. 2. Ehmt1/Ehmt2 activity is responsible for differential H3K9me2 at Foxp3 TSDR by maintaining enhanced levels in Tcon cells. ChIP analyses of H3K9me2 at Foxp3 regulatory regions. FACS-sorted nTreg cells and MACS-purified naïve T cells from male Balb/c mice were compared to *in vitro* differentiated Th1, Th2, and iTreg cells. (a) Enrichment relative to input control is depicted for Foxp3 distal promoter, CNS1, CNS2/TSDR (left) and control regions Il17a promoter, which is enriched for H3K9me2 in all cell types analyzed, and Il2ra intron 1, that shows decreased H3K9me2 after differentiation (right). Data are representative of at least three independent experiments. (b) Naïve cells were treated with or without inhibitor UNC0638 (Unc) during *in vitro* differentiation toward Th1, Th2, and iTreg. Data are representative of at least four independent experiments.

DNA methylation and H3K9me2 are individually regulated at Treg-specific demethylated regions

Next, we studied the impact of vitamin C on the epigenetic remodeling at other TSDRs during iTreg differentiation. We investigated the core set of TSDRs (as defined by Ohkura *et al*. [10]) and exon 6 of Ikzf2 (encoding transcription factor Helios) (Fig. 3c–e). Previous reports have been inconsistent about the role of vitamin C on DNA demethylation at

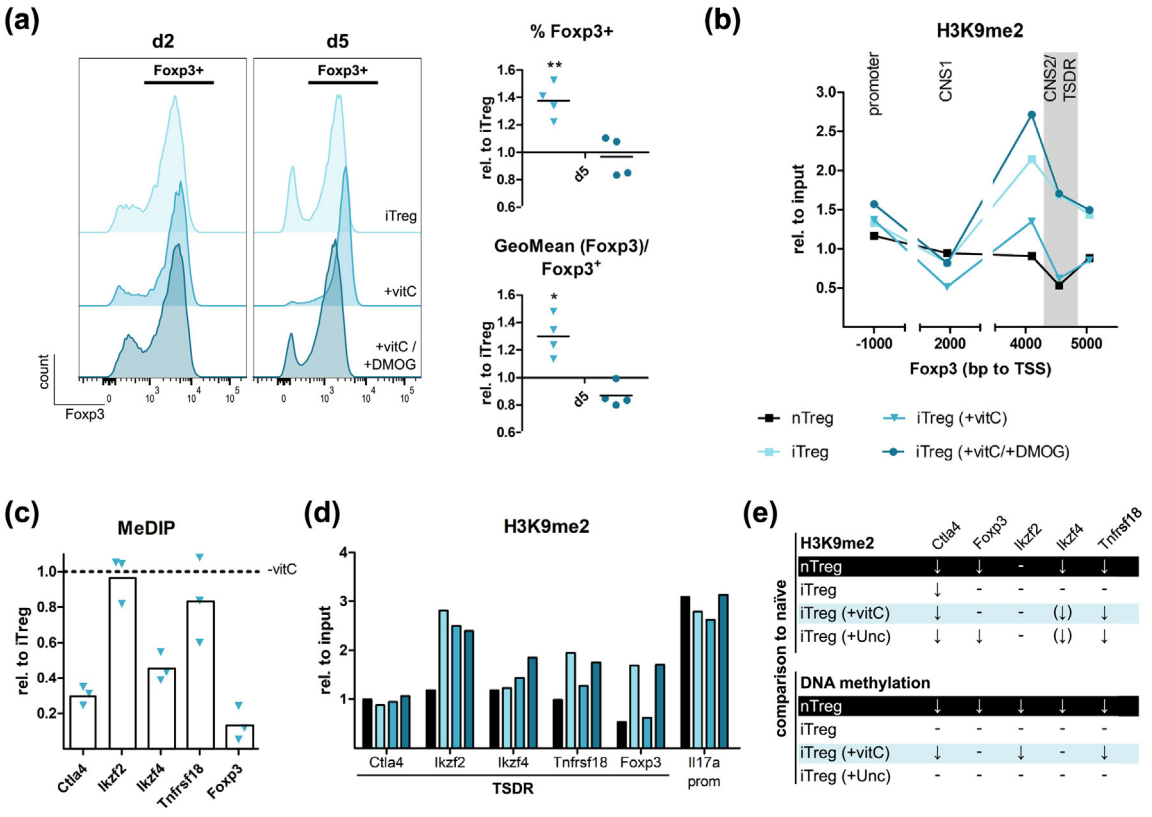

Fig. 3. Vitamin C supplementation mediates epigenetic remodeling at the Foxp3 TSDR and other Treg-specific demethylated regions during iTreg differentiation. FACS-sorted naïve cells from male Foxp3-IRES-GFP mice were differentiated *in vitro* toward iTreg in the absence or presence of vitamin C (+vitC). In addition, the cells were treated with the inhibitor DMOG (or DMSO). (a) Foxp3 was monitored using anti-Foxp3 antibody on days 2 and 5 by flow cytometric analysis (gated on $CD4^+$/alive). Data are depicted exemplarily for one experiment (left) and summarized in scatter plots for day 5 in relation to iTreg cells cultured without vitamin C (left; see Supplementary Fig. S7a for day 2 data). Foxp3 protein levels are presented as geometric mean of Foxp3 intensities in the $Foxp3^+$ fraction. Statistical analysis was performed in relation to iTreg (−vitC) using Student's two-tailed, paired *t* test [* $p < 0.05$; ** $p < 0.01$; n = 2 (d2), n = 4 (d5)]. (b) At the end of culture (d5), iTreg cells were sorted for Foxp3 expression (GFP^+) and H3K9me2 deposition was determined in comparison to nTreg cells at Foxp3 regulatory regions (see Fig. 3d for control region Il17a promoter). Data are representative of 2 (nTreg, iTreg +vitC/+DMOG) or 3 (iTreg, iTreg +vitC) independent experiments. (c) The bar plot depicts DNA methylation levels of TSDRs in iTreg cells cultured in the presence of vitamin C relative to the hypermethylated status in iTreg cells cultured without (−vitC; dashed line) as determined by MeDIP analysis (n = 3). (d) ChIP analysis of H3K9me2 at TSDRs and the control region Il17a promoter. Data are representative of two to three independent experiments as indicated for Fig. 3b. (e) Observations on the epigenetic regulation of DNA methylation and H3K9me2 at TSDRs are summarized and are always in comparison to naïve (arrow marks decrease, − no change). The effects of UNC0638-treatment on epigenetic markers H3K9me2 and DNA methylation were included (Supplementary Fig. S6e and f).

these regions [22,25,26]. In our hands, TSDRs exhibited individual behavior in response to vitamin C supplementation. Foremost, MeDIP analysis confirmed nTreg-specific hypomethylation at all TSDRs investigated and the preserved hypermethylated status in iTreg cells cultured without vitamin C (Supplementary Fig. S6e). In the presence of vitamin C, however, TSDRs of Ctla4 and Ikzf4 exhibited decreased DNA methylation levels. In contrast, TSDRs of Ikzf2 and Tnfrsf18 maintained the hypermethylated status, which is in agreement with data from Yue *et al*. [22] and Nikolouli *et al*. [26] (Fig. 3c).

Similarly, H3K9me2 was individually regulated at TSDRs as revealed by ChIP (Fig. 3d). In detail, H3K9me2 was not differentially deposited at Ikzf4 TSDR. TSDRs of Ctla4, Ikzf2, and Tnfrsf18 showed more or less pronounced H3K9me2 in naïve cells when compared to nTreg cells. However, the high level at Ctla4 TSDR was lost independently of subtype-skewing conditions during *in vitro* differentiation toward Th1, Th2, and iTreg cells. In contrast, H3K9me2 levels at Ikzf2 TSDR were maintained in every condition tested and Tnfrsf18 TSDR was demethylated only in the presence of vitamin C (Fig. 3d and not shown).

Next, we determined the effect of UNC0638 treatment during iTreg differentiation on H3K9me2 at TSDRs. Indeed, H3K9me2 levels decreased in the presence of the inhibitor at all TSDRs that originally exhibited enriched H3K9me2 demonstrating the essential role of histone methyltransferases Ehmt1/Ehmt2 in maintaining H3K9me2 at this set of TSDRs (Fig. 3e, Supplementary Fig. S6f).

Taken together, vitamin C was essential to establish the epigenetic status of DNA hypomethylation and H3K9me2 at several TSDRs. However, whether one or the other element of epigenetic remodeling occurred was not uniformly regulated. Remarkably, apart from Foxp3 TSDR, only those regions showed decreased DNA methylation levels in response to vitamin C that established nTreg-like H3K9me2 levels already in the absence of vitamin C supplementation (i.e., Ctla4 and Ikzf4 TSDRs; Fig. 3e).

Transcription factor Wiz recruits Ehmt1/Ehmt2 to a sequence of Foxp3 TSDR

Ehmt histone methyltransferases do not possess own DNA binding competence. Therefore, we studied how the enzyme complex is recruited to the Foxp3 TSDR in order to maintain H3K9me2. First, we identified the essential binding site within oligo Tsdr(10−12) *via* mutation studies in DNA pull-down experiments. As expected, mutations within Ets1 and Creb1 binding sites blocked binding of the respective transcription factor. In contrast, recruitment of Ehmt1/Ehmt2 was not affected (Fig. 4a, b). *In silico* analysis of the sequence Tsdr(10−12) using the TRAP tool [55] predicted binding of several known CCAAT box (CB)-binding factors, however below the threshold of significance. Nevertheless, mutating two sites with a certain similarity to the CB motif drastically diminished Ehmt1/Ehmt2 recruitment close to background levels (oligo M-CB1; Fig. 4a, b). Additional mutant oligonucleotides demonstrated the importance of one particular CB-like site with the sequence CAATGG (oligos M-CB3/4/5; Fig. 4a, b).

Making use of the unbiased principle of our PD-MS approach, we globally screened for proteins that bind to the CB-like motif. To this end, we compared eluates after DNA pull-down with oligos Tsdr(10−12) and the Ehmt recruitment mutant M-CB3. Overall, 524 proteins were detected in both the forward and reverse samples, 10 of which were enriched by the wt sequence ($|\log_2(H/L)| \geq 1.0$; Fig. 4c; Supplementary Table S1f). As expected, transcription factors Creb1/Atf1 and Ets1 did not bind differentially in the PD-MS screen (Fig. 4d).

Among the enriched proteins, two direct recruiting factors of Ehmt1/Ehmt2 were found, namely, transcription factors *cut-like homeobox 1* (Cux1) and *widely interspaced zinc finger motifs* (Wiz) [56−60] (Fig. 4c, Supplementary Fig. S8b). Both proteins possess binding motifs that show similarity to the CB-like motif of oligo Tsdr(10−12) (Supplementary Fig. S8c). Also, both bound to the various sequence mutants with similar behavior to Ehmt1/Ehmt2 and independently of the DNA methylation status in DNA pull-down (Fig. 4b, d, Supplementary Fig. S8d). Unexpectedly, we found Cux1 to be enriched by the scrambled control oligo (Fig. 4d, Supplementary Fig. S8d). This observation could be explained by a perfect CB motif that was introduced by scrambling (Supplementary Fig. S8a). In line, a second scrambled control was able to prove sequence specific binding of Cux1 to Tsdr(10−12) (scr2; Supplementary Fig. S8a, d). Both proteins, Cux1 and Wiz, are expressed in primary T cells. In fact, Cux1 mRNA increased during *in vitro* differentiation toward iTreg cells but not Th1 cells, which might be ascribed to TGF-β mediated up-regulation of the gene as previously described in NIH3T3 cells [61] (Supplementary Fig. S5b).

To elucidate the role of Cux1 and Wiz in recruiting Ehmt1/Ehmt2 to oligo Tsdr(10−12), we applied CRISPR/Cas to create k.o. clones for the expression of Ehmt1, Ehmt2, Cux1, or Wiz in the RLM-11 cell line (Supplementary Fig. S9a). Subsequent PD-WB analysis with k.o. nuclear extracts demonstrated independent binding of Cux1 and Wiz to oligo Tsdr10−12 (Fig. 5a). Furthermore, the binding of both transcription factors was not altered in the absence of Ehmt1 or Ehmt2. *Vice versa*, Wiz k.o. but not Cux1 k.o. completely abrogated the enrichment of both methyltransferases revealing the essential role of Wiz in recruiting the Ehmt complex. Remarkably, the recruitment appeared to be mediated by an interaction of Wiz with Ehmt1 as k.o. of the latter prevented Ehmt2 enrichment to the same extent as Wiz k.o., whereas Ehmt2 k.o. did not perturb Ehmt1 recruitment (Fig. 5a).

Interaction of Wiz and Ehmt1 is essential for maintenance of H3K9me2 at Foxp3 TSDR and counteracts iTreg differentiation

To investigate the functional relevance of the *in vitro* observed interaction of Wiz and Ehmt1 at oligo Tsdr(10−12) for the epigenetic regulation of Foxp3 TSDR, we used the CRISPR/Cas-generated RLM-11 k.o. clones for ChIP analysis. Noteworthy, wt cells exhibited a comparable H3K9me2 pattern to primary naïve $CD4^+$ T cells at the Foxp3 locus, that is, moderate levels at the distal promoter and CNS1 and a clear enrichment around the TSDR. Double k.o. of Ehmt1 and Ehmt2 drastically decreased H3K9me2 specifically at the Foxp3 TSDR to an overall basic level similar to the effect of chemical inhibition of Ehmt activity in primary T cells (Figs. 2b and 5b).

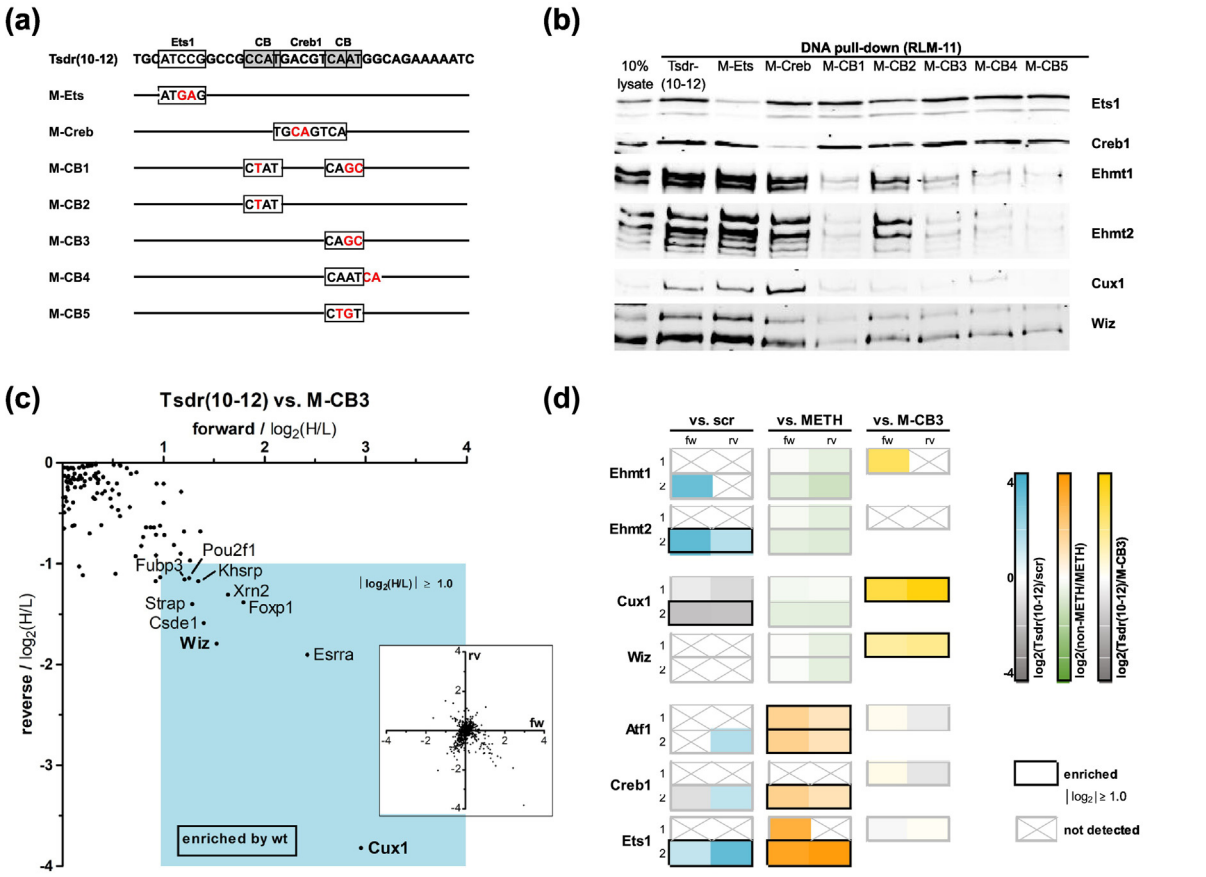

Fig. 4. Ehmt1/Ehmt2 are site-specifically recruited to oligo Tsdr(10−12) by a sequence that mediates binding of transcription factors Cux1 and Wiz. (a and b) Point mutations were introduced into oligo Tsdr(10−12) at binding sites of Ets1 (M-Ets) and Creb1/Atf1 (M-Creb) and sites with similarity to the CCAAT box (CB) motif [M-CB1−5; (a)] to investigate essential nucleotides for the recruitment of Ehmt1/Ehmt2 by PD-WB with nuclear extracts of RLM-11 cells [stimulated with PMA/ionomycin for 5 h; (b)]. Mutant oligos M-CB1/3/4/5 exhibited drastically diminished enrichment of Ehmt1/Ehmt2 proteins. Data are representative of at least two independent experiments. (c) Comparing oligo Tsdr(10−12) to mutant M-CB3, PD-MS with nuclear extracts of SILAC-labeled RLM-11 cells identified 10 proteins specifically enriched by the wildtype (wt) sequence (n = 1). (d) The heat map summarizes PD-MS data of comparisons of oligo Tsdr(10−12) to scr, to the methylated Tsdr(10−12) (*versus* METH) (as presented in Fig. 1), and to mutant M-CB3 for Ehmt1/Ehmt2, Cux1, Wiz, and control proteins (fw forward/rv reverse).

Next, single k.o. clones confirmed the essential role of Ehmt1 and Wiz for H3K9me2 at the Foxp3 TSDR in RLM-11 cells, whereas Cux1 k.o. and Ehmt2 k.o. did not alter H3K9me2 levels (Fig. 5b). However, DNA methylation levels were maintained in all clones as assessed by MeDIP analysis and bisulfite sequencing (Supplementary Fig. S9b, c). In addition, CRISPR/Cas-mediated double k.o. of Ehmt1/Ehmt2 or Wiz k.o. clearly decreased H3K9me2 also at other TSDRs (Supplementary Fig. S9d). Even at regulatory regions of the cytokine genes Ifng (Th1), Il4 (Th2), Il17 (Th17), and Il10 (Th1/Th17), maintenance of H3K9me2 was dependent on the interaction of Wiz and Ehmt1 in the RLM-11 cell line (Supplementary Fig. S9e, f).

To confirm the role of the Wiz−Ehmt1 interaction in primary T cells, we applied the CRISPR/Cas technique with the approved guide RNA pairs targeting Ehmt1, Ehmt2, Cux1, or Wiz during iTreg differentiation. Positively transfected cells (expressing the reporter GFP) and not positively transfected (GFP^-) fractions were expanded for two consecutive differentiation rounds under iTreg-skewing conditions. In these CRISPR/Cas-treated batch cultures, target gene expression was decreased to approx. 50% as determined by RNA quantification or WB analysis (Supplementary Fig. S10a, b).

Despite the partial k.o., ChIP analysis of H3K9me2 confirmed the role of both Wiz and Ehmt1 at Foxp3 TSDR in primary cells: while targeting Cux1 had no impact on the epigenetic mark, targeting of Ehmt1 and especially Wiz resulted in the reduction of H3K9me2 (Fig. 5c). In contrast to RLM-11 clones, targeting Ehmt2 in primary cells also decreased

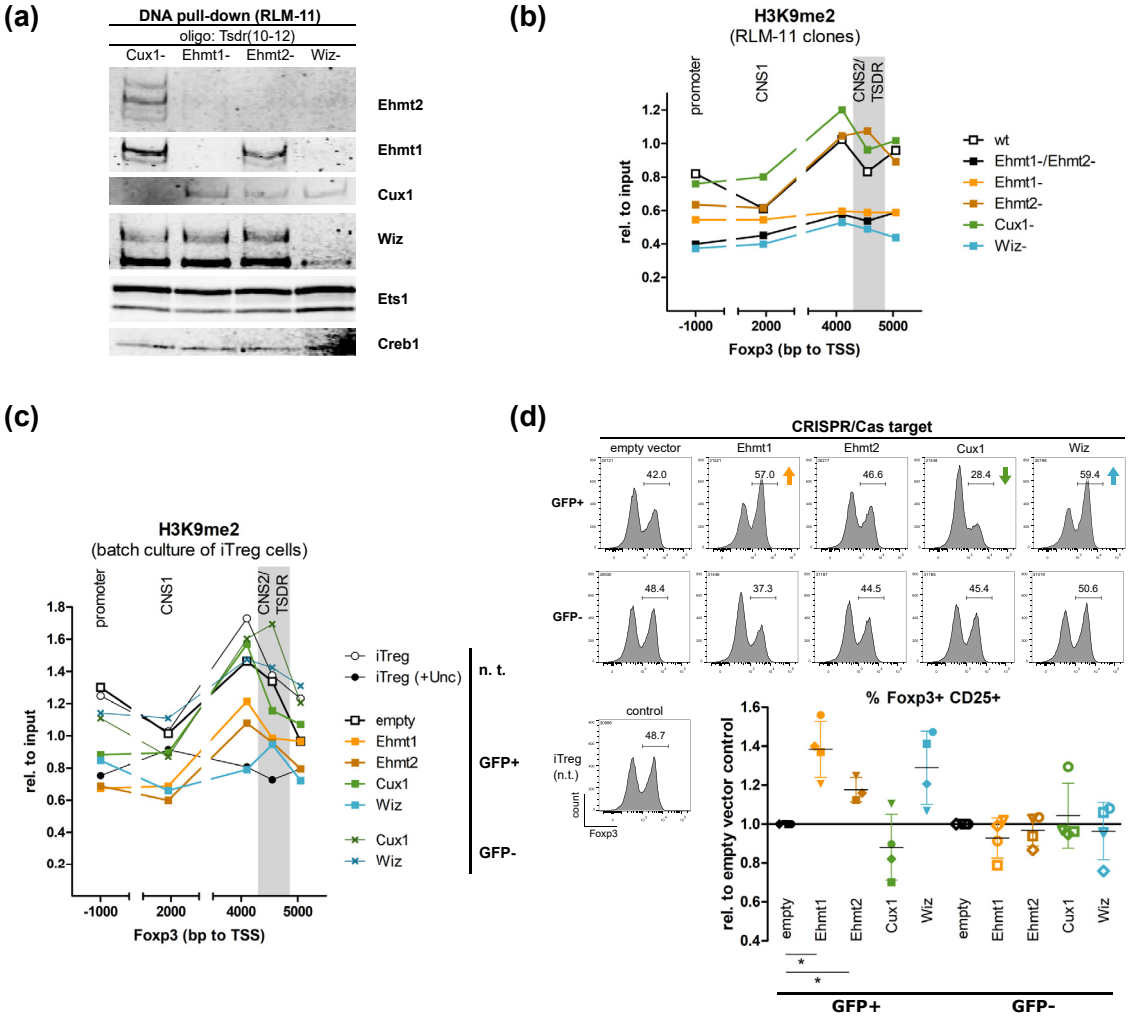

Fig. 5. Transcription factor Wiz recruits Ehmt1/Ehmt2 to the Foxp3 TSDR to maintain H3K9me2. (a) PD-WB was performed with oligo Tsdr(10−12) and nuclear extracts of RLM-11 k.o. clones (stimulated for 5 h with PMA/ionomycin) with deficiency of Ehmt1, Ehmt2, Cux1, or Wiz that were generated *via* CRISPR/Cas-mediated gene editing (n = 3). (b) H3K9me2 deposition at Foxp3 regulatory regions was determined in RLM-11 k.o. clones by ChIP. Data are representative for two to three replicates of the presented clone and two different clones investigated for each CRISPR/Cas target in independent analyses. Control regions Junb promoter and Rhox11 promoter are shown in the corresponding Supplementary Fig. S9e. (c and d) The CRISPR/Cas technique was applied for gene editing of Ehmt1, Ehmt2, Cux1, and Wiz to interfere with expression in primary T cells. MACS-purified naïve $CD4^+$ T cells from male C57Bl6N (3 exp.) or DO11.10xBalb/c (1 exp.) mice were transfected with genomic information for Cas9 nickase and specific pairs of guide RNAs or Cas9 nickase alone (empty vector control) on day 2 of *in vitro* differentiation toward iTreg. Positively (GFP^+) and negatively transfected cells (GFP^-) were separated by FACS and expanded for two consecutive rounds of iTreg differentiation, which resulted in iTreg batch cultures with or without partial knockout of the targeted gene, respectively. In parallel, not transfected (n.t.) cells were cultured with or without the inhibitor UNC0638 (Unc). (c) CRISPR/Cas-targeted batch cultures of primary iTreg cell cultures were examined for H3K9me2 deposition at Foxp3 regulatory regions by ChIP. Data are representative of two independent experiments. Control regions are shown in the corresponding Supplementary Fig. S10c. (d) At the end of culture, ratios of $Foxp3^+$ $CD25^+$ cells (gated on $CD4^+$) were determined by flow cytometry. Exemplary data for one experiment are shown as determined by anti-Foxp3 antibody (top). Results of three to four independent biological replicates (pooled primary cells from four to five mice, each) are indicated by distinct symbols (○/● DO11.10xBalb/c) and are summarized in the scatter plot (mean ± SD; bottom). Depicted are $Foxp3^+$ $CD25^+$ ratios of $CD4^+$ cells relative to the respective empty vector control (GFP^+/GFP^-). Data points of one particular experiment that exhibited overall higher $Foxp3^+$ $CD25^+$ ratios are marked by triangles. Statistical analysis was performed in relation to the respective empty vector control using Student's two-tailed, paired *t* test (* $p < 0.05$). For GFP^+ samples, *p* values were 0.013 (Ehmt1), 0.040 (Ehmt2), 0.254 (Cux1), and 0.054 (Wiz).

H3K9me2 levels at the Foxp3 TSDR (Fig. 5c), which may be attributable to decreased Ehmt1 protein levels in these cultures. In fact, an interdependency of Ehmt1 and Ehmt2 protein stabilities has been described previously in ES cells [30,57]. In accordance, one particular Ehmt2 k.o. clone (RLM-11 cell line) also exhibited decreased Ehmt1 protein levels and correspondingly decreased H3K9me2 at the Foxp3 TSDR (Supplementary Fig. S9 g, h). However, we cannot exclude a subordinate role of Ehmt2 in the epigenetic regulation of the Foxp3 TSDR.

In line with the altered histone methylation, we observed altered Foxp3 expression in a guide RNA-specific manner. In three out of four CRISPR/Cas experiments, targeting Ehmt1 or Wiz resulted in an increase of about 20%–50% of Foxp3$^+$ CD25$^+$ cells when compared to empty vector control indicating an important role for Ehmt1 and Wiz in iTreg cell differentiation. *Vice versa,* targeting of Cux1 led to a decrease of 10%–30%, while non-positively transfected (GFP$^-$) cells were not affected (Fig. 5d). The divergent fourth experiment, which showed no clear guide RNA-specific effect, also differed in overall higher ratios of Foxp3$^+$ CD25$^+$ cells in all cultures (>60%; Supplementary Fig. S10d), indicating that Ehmt1, Wiz, and Cux1 may have a more significant impact on Foxp3 expression under suboptimal differentiation conditions.

Taken together, transcription factor Wiz exhibited a crucial role in mediating enzyme activity of histone methyltransferase Ehmt1 to Foxp3 TSDR. This mechanism appears to be essential for creating a repressive epigenetic landscape by deposition of the histone mark H3K9me2. Remarkably, CRISPR/Cas targeting of Wiz or Ehmt1 in iTreg cells favored Foxp3 expression, which corresponds well with the stabilizing function of the TSDR in Foxp3 expression.

Discussion

The stability of Foxp3 expression is fundamentally regulated *via* the epigenetic landscape of the Foxp3 TSDR. In particular, the DNA methylation status has been shown to be a reliable indicator for the region's activity [4,5,14,15]. However, other levels of epigenetic regulation at the Foxp3 TSDR and underlying molecular mechanisms are widely undiscovered.

Here, we provide several lines of evidence that histone methyltransferase Ehmt1 is a crucial epigenetic regulator of the Foxp3 TSDR and impacts on Treg differentiation. First, using an unbiased DNA pull-down approach, we showed that the Ehmt enzyme complex is recruited to a functional element of the Foxp3 TSDR, where it exhibits a preference for the methylated state (Tcon characteristic). Second, we observed elevated H3K9me2 levels at the Foxp3 TSDR in Tcon cells that were essentially dependent on the enzymatic activity of Ehmt proteins as demonstrated by the application of specific inhibitors. Conclusively, knockout of Ehmt1 diminished H3K9me2 at this region in the RLM-11 cell line and primary T-cell cultures. Third, during Treg differentiation, the epigenetic remodeling of the Foxp3 TSDR involves erasure of H3K9me2, which can be monitored in iTreg cells induced under vitamin C supplementation. Accordingly, administration of DMOG, an inhibitor of histone demethylases and Tet enzymes, abolished vitamin C-induced demethylation of H3K9me2 at the Foxp3 TSDR, indicating an active remodeling mechanism. Fourth, CRISPR/Cas-mediated knockout of transcription factor Wiz abolished Ehmt recruitment to Tsdr(10–12) in DNA pull-down experiments and interfered with the maintenance of H3K9me2 at the Foxp3 TSDR, revealing that Wiz is essential for the recruitment and function of the Ehmt complex at this region. Finally, CRISPR/Cas targeting of Wiz or Ehmt1 during differentiation of iTreg cells increased the number of Foxp3$^+$ cells, indicating an essential and repressive role of the Wiz–Ehmt1 interaction in iTreg differentiation. A graphical summary is given in Fig. 6.

To our knowledge, the role of Ehmt1 in T cells has not yet been addressed. Specific deletion of Ehmt2 in T cells, however, resulted in an unexpectedly mild phenotype [62]. These mice showed no alterations in T lymphocyte development [63]. Furthermore, although promoters and other regulatory regions of the lineage-determining cytokines IFNγ, Il-4, and Il-17α exhibited Ehmt2-dependent H3K9me2, Ehmt2 deficiency in T cells did not result in promiscuous gene expression *per se* [64]. These observations were in stark contrast to ES cells, where Ehmt2 deficiency demonstrated the enzyme's crucial role during imprinting and embryonic development [36,39–42]. Our data support the observation of previous reports that Ehmt2 appears to have a minor role in controlling the epigenetic status of the Foxp3 TSDR [65].

Based on findings in ES cells, it was originally assumed that Ehmt1 and Ehmt2 generally function as a heterodimeric complex to fulfill enzymatic activity [30]. Only recently have the heterodimer-independent functions for both enzymes been described as well, in particular in largely differentiated cell types, that is, brain tissue and during terminal differentiation of myoblasts toward skeletal muscle cells [66,67]. It is tempting to speculate that in the course of differentiation, Ehmt1 and Ehmt2 may have gained specialized and individual functions in differentiation programs of cells arising from the same progenitor. In a very recent report, Ehmt2 was shown to be crucial for CD8$^+$ T-cell differentiation by repressing typical Th cell-associated genes, for example, Cd4 [68]. Strikingly, we found Ehmt1 to be essential for the deposition of H3K9me2 at

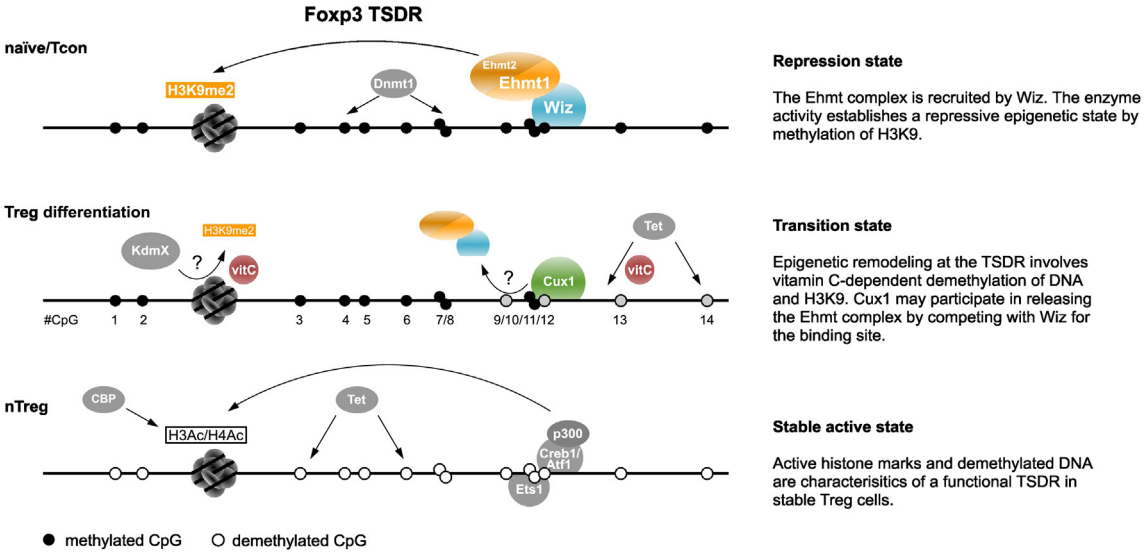

Fig. 6. Epigenetic regulation at the Foxp3 TSDR by Ehmt activity during Treg differentiation. The model illustrates the action of the Wiz−Ehmt complex investigated in this study (colored elements) and puts it into the context of previously described epigenetic mechanisms that control the DNA methylation state of the region, for example, Tet-mediated demethylation (grayscale elements). Speculative assumptions that were raised by the presented data are emphasized by interrogation mark.

various TSDRs including the Foxp3 gene and additionally at lineage-determining cytokine loci, which are regulated by differential DNA methylation. Thus, our data indicate a predominant role of Ehmt1 in Th cell differentiation programs and suggest a cooperation of H3K9me2 and DNA methylation in a systemic fashion, as has been described in differentiation programs of ES cells [36].

In line with a previous report that demonstrated direct interaction of Wiz and Ehmt1 in 293T cells using co-immunoprecipitation [59], the recruitment of Ehmt1 to oligo Tsdr(10−12) was mediated *via* interaction with transcription factor Wiz and independently of Ehmt2.

Degeneracy of transcription factor binding sites is a frequently observed phenomenon. Thus, the similarity of the WIZ binding motif with the sequence of oligo Tsdr(10−12), which contains the essential bases for Wiz interaction, indicates direct binding of the transcription factor to the sequence. However, we cannot exclude the possibility that other proteins may be involved in the recruitment of Ehmt1/2 to oligo Tsdr(10−12). The presumed Wiz binding site is conserved between mouse and human. Accordingly, we detected human WIZ to bind to the human sequence (Supplementary Fig. S11). It therefore seems likely that cooperative regulation by DNA methylation and H3K9me2 is an evolutionarily conserved mechanism to epigenetically close the Foxp3 TSDR in non-Treg cells.

Using DNA pull-down experiments, we identified the transcription factor Cux1 to bind to the same binding site within Tsdr(10−12) that was essential for Ehmt recruitment. Also, Cux1 appeared to show stronger enrichment by the mutant M-Creb. The mutation of M-Creb is surrounded by DNA bases that were found to be essential for the binding of Cux1 to Tsdr(10−12). The stronger enrichment may be attributable to the lack of competition with other factors that are impaired in binding to the mutated sequence (e.g., Creb1 itself). Alternatively, the alteration of the DNA sequence may enhance binding affinity of Cux1. Although Cux1 has been shown to directly interact with Ehmt2 [56], we found no hint that Cux1 participates in the recruitment of the Ehmt complex to the Foxp3 TSDR. On the contrary, CRISPR/Cas-mediated deficiency of Cux1 appeared to stabilize H3K9me2 levels at this site as well as at certain other investigated Ehmt target sites. Moreover, Cux1 appeared to positively affect iTreg differentiation as seen by the reduced number of Foxp3$^+$ cells due to CRISPR/Cas targeting of Cux1, which was in contrast to the action of Wiz and Ehmt. Thus, we hypothesize that Cux1 could displace the Wiz−Ehmt complex from the TSDR during Treg differentiation, allowing for effective and enzymatically driven H3K9me2 demethylation and the opening of the region (Fig. 6). Strikingly, Cux1 expression has been shown to be enhanced by TGF-β1 stimulation [61] and accordingly was upregulated during iTreg differentiation. Interestingly, displacement of competing transcription factors in order to reverse expression control has already been shown for Cux1 in other contexts [69−73].

Most recently, vitamin C has been found to be essential for DNA demethylation of Foxp3 TSDR by Tet enzymes [22,25]. In contrast, vitamin C supplementation benefits Th17 cell differentiation in a Tet-independent manner *via* enhanced H3K9 demethylation by Jmjd2 (Kdm4) enzymes [74]. Similarly, our observations at the Foxp3 TSDR point to an actively catalyzed demethylation of H3K9me2, presumably by Kdm3/Kdm4 enzymes, as can be hypothesized from the dependency on vitamin C as well as inhibition studies with the 2OG-analogon DMOG. However, the molecular conservation of the catalytic principal of Tet enzymes and H3K9me2 demethylases impedes an immediate investigation to address this question due to the lack of specific inhibitors. Further investigation depends on the identification of the demethylase responsible for H3K9me2 demethylation at the Foxp3 TSDR. Subsequent directed loss-of-function studies may have the potential to elucidate the mechanisms guiding the epigenetic remodeling with regard to H3K9 and DNA demethylation and any potential interconnection at this region.

Both vitamin C and the 2OG-analogon DMOG act mechanistically on the enzyme activity of Fe(II)- and 2OG-dependent dioxygenases, which include not only Kdm histone demethylases and Tet enzymes but also hydroxylases. In particular, vitamin C-dependent hydroxylation of the alpha subunit of hypoxia-inducible factor (HIF1α) has been shown to control transcriptional activity of HIF1 on its gene targets and has been brought into the context of immune cell function and metabolism [75–77]. Although the experiments presented here were performed under normoxic conditions, we cannot exclude that altered HIF1 activity may be involved in the overall effect of vitamin C supplementation on iTreg differentiation by altering the expression in iTreg cells. However, vitamin C supplementation was found to leave the transcriptome of alloantigen-induced iTreg cells mostly unaffected [26]. Furthermore, the impact of vitamin C on epigenetic programs in general is thought to be mainly attributable to enhanced enzyme activity of Tet DNA demethylases and Kdm histone demethylases rather than HIF1 [77].

Our data point to co-regulation of H3K9me2 and the DNA methylation status at the Foxp3 TSDR. nTreg cells that stably express Foxp3 are devoid of both H3K9me2 and DNA methylation at this region. In contrast, both marks are actively maintained during *in vitro* differentiation of Tcon cells and iTreg cells that show unstable Foxp3 expression. The addition of vitamin C, which mediates stable Foxp3 expression [22], was sufficient and necessary to stimulate the Treg-specific epigenetic remodeling on both epigenetic levels in iTreg cells. Hence, H3K9me2 and DNA methylation might act in a cooperative manner to create a repressive epigenetic landscape at the Foxp3 TSDR and to control the stability of Foxp3 expression (Fig. 6).

In addition to Foxp3 TSDR, we observed a co-occupancy by DNA methylation and H3K9me2 at other TSDRs. However, the epigenetic remodeling of TSDRs was not uniformly regulated. In fact, different stimuli were required to induce the Treg-specific epigenetic status on the level of DNA methylation and H3K9me2 at individual TSDRs during iTreg differentiation. Still, vitamin C was a significant factor. Recent studies were inconsistent concerning the role of vitamin C in the epigenetic remodeling of TSDRs [22,25,26]. As we observed vitamin C-mediated DNA demethylation at TSDRs of Ctla4, Ikfzf4, and Foxp3, our results are in line with Yue *et al*. [22] and Nikolouli *et al*. [26]. Interestingly, DNA demethylation of Ctla4 and Ikfzf4 TSDRs was found to occur independently of Foxp3 expression in alloantigen-induced iTreg cultures [26], which raises the question of whether epigenetic remodeling at these sites occurs specifically in Treg cells when vitamin C is available. In fact, we could not find evidence for vitamin C-mediated DNA demethylation of either TSDR when naïve cells were differentiated toward Th1 (not shown). This suggests a mechanism that requires Treg-skewing signals to enable DNA demethylation of Ctla4 and Ikfzf4 TSDRs. Nevertheless, vitamin C supplementation was not sufficient to induce complete Treg-specific epigenetic remodeling as observed for TSDRs of Tnfrsf18 and Ikzf2.

By identification of the Wiz–Ehmt1 interaction in Th cells and its role for H3K9me2 deposition at the Foxp3 TSDR, we discovered and characterized the second epigenetic mechanism to maintain the repressive landscape of the region in Tcon cells. Thus, our findings contribute to the understanding of how Foxp3 expression, and therefore the differentiation of Treg cells, is epigenetically controlled. In agreement with recent reports [22,25,26], our data confirm the need for vitamin C to enable Treg-specific epigenetic remodeling of the Foxp3 locus and other TSDRs. Importantly, the necessity of vitamin C for a whole class of ubiquitous epigenetic regulators highlights the need for controlled and adequate supplementation *in vitro* in various experimental settings across tissues and cell types.

Materials and Methods

Mice and cell lines

Foxp3-IRES-GFP [78], BALB/cJ-Tg(DO11.10), and C57BL/6NJ mice were bred under pathogen-free conditions in the animal facility of the Federal Institute for Risk Assessment (Berlin, Germany). Non-transgenic C57BL/6NCrl (strain code 027) and

BALB/cAnNCrl mice (strain code 028) were purchased from Charles River (Sulzfeld, Germany).

The murine $CD4^+$ $CD8^-$ thymoma T-cell line RLM-11 was cultivated in Glutamax RPMI 1640 medium (Gibco) supplemented with 10% FCS, 100 U/ml penicillin, 100 U/ml streptomycin, and 10 μg/ml β-mercaptoethanol.

DNA pull-down

Nuclear extracts were prepared from RLM-11 cells stimulated with 10 ng/ml phorbol 12-myristate 13-acetate (PMA; Sigma-Aldrich) and 1 μg/ml Ionomycin (Merck) for 5 h using the Nuclear Extract Kit (Active Motif). Fifty micrograms of nuclear extract was pre-incubated with 5 μg poly(dI-dC) (Sigma) in 400 μl binding buffer [17] supplemented with 1 mM DTT and 1 × cOmplete protease inhibitor cocktail (Roche) for 1 h. Streptavidin agarose (25 μl; Sigma) was loaded with 200 pmol biotinylated ds oligonucleotide (Supplementary Table S2b) in 400 μl binding buffer for 1 h. Subsequently, washed agarose beads were incubated with protein extract for 4 h at 4 °C. Complexes were washed twice with 1 ml binding buffer followed by 1 ml 50 mM NH_4HCO_3, twice. For Western blot analysis, samples were eluted with 25 μl 2 × SDS loading buffer [79] at 95 °C for 5 min.

Where stated, oligonucleotides were cleared from ss molecules before DNA pull-down by S1 nuclease treatment (60 U/μmol of oligonucleotide) for 30 min at 37 °C. The reaction was stopped by addition of 33 mM EDTA.

Immunoblotting

Immunoblotting was performed as previously described [80] using discontinuous SDS-PAGE and the Odyssey system (LiCOR). For total protein analysis, cells were resuspended in 2 × SDS loading buffer. Antibodies used for Western blot analysis were as follows: anti-Ehmt1 (B0422; Abcam); anti-Ehmt2 (A8620A; Invitrogen); anti-Kdm3a (PA5−23066), anti-Wiz (PA5-21082; Thermo Fisher Scientific); anti-Foxp3 (FJK-16s; eBioscience); anti-Creb1 (48H2), anti-Yy1 (13G10; Cell Signaling Technology); anti-Atf1 (H-60), anti-Cstf2 (H-300), anti-Cux1 (B-10), anti-Elf1 (C-20), anti-Ets1 (C-20), anti-Gabpα (H-180); anti-Lamin B (M-20), anti-Nfyα (H-209), anti-Oct1 (C-21), anti-Ptbp (N-20), anti-Rfx1 (H-230), anti-Tgif1 (H-172; all Santa Cruz Biotechnology); anti-Tbet (4B10; BioLegend); and anti-NFATc2 (rabbit pAb; DRFZ Berlin). IR-DYE coupled secondary antibodies from donkey were obtained from LiCOR.

DNA pull-down with mass spectrometric analysis (PD-MS)

RLM-11 cell cultures were differentially labeled applying stable isotope labeling by amino acids in cell culture (SILAC) [44,81]. SILAC media were prepared from complete RPMI 1640 medium (lacking arginine and lysine) by supplementation of 0.115 mM light ($^{12}C/^{14}N$) or heavy ($^{13}C/^{15}N$) arginine and 0.275 mM light or heavy lysine, respectively. Light L-proline (2.6 mM) was added to all media to avoid arginine-to-proline conversion [82]. RLM-11 cells were grown in heavy or light SILAC medium for at least 10 days (18−20 cell divisions). Before nuclear extract preparation, cultures were stimulated with PMA and ionomycin and nuclear extracts were prepared as described above. For downstream mass spectrometric analysis, DNA pull-down samples were eluted by pH shift using 25 μl of 50 mM NH_4HCO_3 (pH 10). Differentially labeled eluates of Tsdr(10−12) and the sequence to be compared were pooled from 4 single samples, each. Subsequently, the total volume was narrowed to <20 μl by vacuum evaporation and samples were prepared for mass spectrometry by in-solution-digestion following standard procedures. Briefly, 20 μl of urea buffer [6 M urea, 2 M thiourea, 10 mM Hepes (pH 8.0)] was added, followed by reduction with DTT and alkylation with iodoacetamide. Digestion was performed using LysC for 3 h at room temperature, followed by trypsin overnight (after diluting samples to less than 2 M urea). Samples were acidified with TFA and peptides were extracted and desalted using STAGE tips. LC−MS/MS was performed on using a 240-min acetonitrile gradient using 20-cm-long reversed phase columns (fritless, 75 μm ID, packed in-house with 3 μm ReproSil-Pur C18-AQ) on a Proxeon HPLC system (Thermo) coupled online to a QExactive Plus mass spectrometer (Thermo). The mass spectrometer was operated in the data-dependent mode with a resolution of 70,000 for full scans (AGC target 1E6) and up to 10 MS2 scans (resolution 17,500; AGC target 1E5; maximum IT = 60 ms; dynamic exclusion for 30 s; excluding singly charged peaks and peaks with unassigned charge states). Raw files were analyzed using MaxQuant (version 1.5.3.18) with default parameters and searched against a mouse protein databases (uniprot.MOUSE.2012-06 and uniprot.-MOUSE.2014-10) plus common contaminants with a false-positive rate of 1% at both the protein and peptide level. Reverse database hits, contaminants, and proteins only identified by site were discarded.

CD4 T-cell isolation and *in vitro* differentiation cultures

$CD4^+$ $CD25^-$ cells were prepared from mixed murine splenocytes and lymph node cells by magnetic cell sorting (MACS). After lysis of erythrocytes, cells were depleted for CD25 using anti-CD25-APC (PC61.5, eBioscience) and anti-APC

MicroBeads (Miltenyi Biotec). Subsequently, cells were MACS-sorted for CD4 using anti-CD4 MicroBeads (L3 T4, Miltenyi Biotec).

Alternatively, $CD4^+$ $CD25^-$ $CD44^{low}$ $CD62L^{high}$ (GFP^-) naïve cells were prepared from mixed murine splenocytes and lymph node cells by FACS using a FACSAria II (BD Biosciences). Prior to that, the $CD4^+$ cell fraction was enriched by MACS using rat anti-CD8 (53-6.72), anti-B220 (RA3.6B2), and anti-Mac1 (M1/70.15.11; all DFRZ Berlin) and anti-rat MicroBeads (Miltenyi Biotec). Enriched fractions were labeled with anti-CD4-PE (GK1.5; DRFZ Berlin), anti-CD44-PacB (IM7), anti-CD62L-PE-Cy7 (MEL-14), and anti-CD25-APC (PC61.5, all eBioscience).

For *in vitro* differentiation, MACS-sorted $CD4^+$ $CD25^-$ or FACS-sorted naïve cells were cultured in complete RPMI 1640 medium (10% FCS, 10 μg/ml β-mercaptoethanol, 100 U/ml penicillin/streptomycin, 50 μg/ml gentamicin) in the presence of subtype-skewing supplements, that is, 10 ng/ml rmIL-12, 10 ng/ml rmIL-2, and 10 μg/ml anti-IL-4 (11B11) for Th1; 40 ng/ml rmIL-4, 10 ng/ml rmIL-2, 10 μg/ml anti-IL-12 (C17.8), and 10 μg/ml anti-IFNγ (AN18.17.24; all DRFZ Berlin) for Th2; and 10 ng/ml rmIL-2, 2 ng/ml pTGF-ß1, 10 μg/ml anti-IFNγ, 10 μg/ml, anti-IL-4 for iTreg. Cells were cultured for 48 h with plate-bound anti-CD3e (145-2C11) and anti-CD28 (37.51; both DRFZ Berlin) and then taken from the stimulus adding fresh medium and 10 ng/ml rIL-2 for another 3 days. Cultures were harvested, and either FACS-sorted for living (DAPI) and GFP or dead cells were removed from cultures using density gradient centrifugation.

nTreg cells were prepared as described for naïve cells and were isolated *via* FACS for $CD4^+$ $CD25^+$ (GFP^+). nTreg cells were cultured *in vitro* in the presence of 50 ng/ml rmIL-2 as described above.

Inhibitors BIX-01294, dimethyloxalylglycine (DMOG), and UNC0638 (all Cayman) were dissolved in DMSO and diluted at least 1:2000 in cell culture to yield a concentration of 1, 67, and 1 μM, respectively. Vitamin C (L-ascorbic acid) was purchased from Sigma-Aldrich and dissolved in sterile water. Vitamin C was given to cell cultures in a concentration of 20 μg/ml.

Treg *in vitro* stability assay and flow cytometric analysis

For the *in vitro* stability assay, harvested iTreg cells were sorted for $DAPI^-$ GFP^+ and were cultured for another round of *in vitro* differentiation as described above but lacking pTGF-ß1. After 5 days, living $CD4^+$ cells were monitored for CD25 and Foxp3 protein levels by flow cytometry.

For flow cytometric analysis, cells were stained with 67 μM NHS-PacO (Thermo Fisher Scientific) for live/dead discrimination and fixed with the Foxp3 fixation/permeabilization buffer (eBioscience) according to the manufacturer's instructions. All presented flow cytometric data regarding Foxp3 were determined by anti-Foxp3 antibody. Antibody species used for flow cytometric analysis were anti-Foxp3-PE-Cy7 (FJK-16 s), anti-CD25-APC (PC61.5; both eBioscience), and anti-CD4-PE or -FITC (GK1.5, DRFZ Berlin). Flow cytometric analysis was carried out on an LSRII (BD Biosciences).

CRISPR/Cas9n in primary cells during iTreg differentiation

The CRISPR/Cas9 nickase vector pSpCas9n(BB)-2A-GFP (PX461) was a gift from Feng Zhang (Addgene plasmid 48,140) [83]. Guide RNA pairs targeting the first exon expressed by all isoforms of the respective gene were designed by the help of CRISPR Design (Massachusetts Institute of Technology). Guide RNA sequences were synthesized with adequate overhangs for cloning with BpiI and were inserted into the vector as previously described by Ran *et al*. [83] (Supplementary Table S2c). Correct insertion was confirmed by Sanger sequencing.

For transfection, *in vitro* iTreg cultures were prepared as described above. Forty-eight hours after primal stimulation, cultures were transfected with the respective pair of target-specific plasmids using the Neon transfection system (Thermo Fisher). In detail, 2×10^6 cells were transfected with 10 μg of each plasmid or 20 μg of the empty vector in 100 μl buffer R applying double pulsing for 20 ms each at 1350 V. Subsequently, *in vitro* iTreg culture was continued with TCR stimulation for additional 24 h in antibiotic-free medium including subtype-skewing supplements. Antibiotics were added 6 h after transfection. The cells were cultured for another 24 h without TCR stimulation before sorting the populations on the basis of GFP expression by FACS. Transfection efficiencies varied between experiments from 6% to 13% of GFP^+ cells within the viable cell populations. Fractions were incubated in original medium supplemented with fresh rmIl-2 (10 ng/ml) for another 24 h. Two consecutive rounds of standard *in vitro* iTreg culture were performed to expand CRISPR/Cas9n-treated cell populations. Finally, cells were harvested using density gradient centrifugation for subsequent analyses.

Establishment of RLM-11 k.o. clones using CRISPR/Cas9n

RLM-11 cells (2×10^6) were transfected with 1 μg each of the pair of target-specific CRISPR/Cas9n plasmids *via* electroporation using the Cell Line Nucleofector Kit L (Lonza). Positively transfected

cells were FACS-sorted as single cells by the expression of GFP. Established clones were tested for perturbed expression of the target gene by Western blot analysis (Fig. S8A).

Chromatin immunoprecipitation

ChIP assays were performed according to the chromatin immunoprecipitation (ChIP) assay by Miltenyi Biotec. Briefly, cells were fixed with 1% formaldehyde for 5 min at RT. Per sample, 2×10^6 cells were lysed in 50 μl ChIP lysis buffer [50 mM Tris−HCl (pH 8.1), 10 mM EDTA, 1% SDS, 1 × cOmplete protease inhibitor cocktail (Roche)]. The reaction was stopped by adding 150 μl ChIP dilution buffer [16.7 mM Tris−HCl (pH 8.1), 1.2 mM EDTA, 167 mM NaCl, 1.1% Triton X-100, 0.01% SDS, 1 × cOmplete protease inhibitor cocktail], and DNA was sheared using the Sonopuls Ultrasonic homogenizer (5 × 8 s at 20% intensity; Bandelin electronic). Debris was centrifuged at 13,000*g*, and 150 μl of extract was incubated with 2 μg anti-H3K9me2 (1220; Abcam) or anti-H3K9ac (pAb; Active Motif) at 4 °C overnight. Ten percent of extracts were saved as input control. ChIP samples were incubated with Protein A MicroBeads for 1 h followed by extensive washing on MACS separation columns (Miltenyi Biotec). Immunoprecipitated chromatin was reverse-crosslinked with 200 mM NaCl at 65 °C for 4 h. Immunoprecipitated DNA was purified with the DNA extract II kit (Macherey and Nagel). The relative enrichment of specific DNA sequences over input was determined by real-time PCR with the Mx3000 system (Stratagene) using QuantiTect SYBR Green RT-PCR Kit (Qiagen). Primer sequences are listed in Supplementary Table S2a.

Bisulfite sequencing and MeDIP

DNA was prepared using the QIAamp DNA Mini Kit (Qiagen). Bisulfite sequencing was performed by Varionostic (Ulm, Germany). Methylated DNA precipitation (MeDIP) analysis was performed as described for ChIP with the following modifications: 1.5 μg of total genomic DNA was sonicated in 225 μl AE buffer (Qiagen). One hundred fifty microliters of sheared DNA was denatured for 10 min at 95 °C, rapidly cooled down and incubated with 100 μl MeDIP buffer (25 mM Na_3PO_4 (pH 7), 350 mM NaCl, 0.125% Triton X-100), and 2 μg anti-5′-methyl-cytidine antibody (33D3, Eurogentec) overnight. Incubation with Protein A MicroBeads and purification were carried out as described for ChIP.

RNA expression analysis

RNA was extracted using the Total RNA Purification kit (Norgen). Reverse transcription was performed using Superscript II reverse transcriptase (Invitrogen) and oligo-dT primer according to the manufacturer's protocol. Quantification of RNA species was determined by real-time PCR relative to the housekeeping gene *rps18.* Primer sequences are provided in Supplementary Table S2a.

Supplementary data including further information on PD-MS technique and detailed MS data can be found online.

Acknowledgment

We thank Alf Hamann and Julia Polansky-Biskup (DRFZ Berlin) for kindly giving access to a previously established protocol for bisulfite-based DNA methylation analysis of Foxp3 TSDR. We thank Patrick Pankert and Thermo Fisher for technical advice and MS analysis of samples (experiment 2). We thank Eliot Morrison for proofreading of main excerpts of the manuscript. We also thank Timo Lischke, Manja Jargosch, and Stefanie Gryzik for discussions and helpful advice. This study was funded by the DFG (Deutsche Forschungsgemeinschaft) Grant SFB 650 (to R.B.) and by the BMBF (German Federal Ministry of Education and Research) as part of the project eBio: T-Sys (to R.B. and A.R.).

Declaration of Competing Interest

The authors declare no conflict of interest.

Appendix A. Supplementary data

Supplementary data to this article can be found online at https://doi.org/10.1016/j.jmb.2019.07.031.

Received 29 January 2019;
Received in revised form 13 July 2019;
Accepted 17 July 2019
Available online 27 July 2019

Keywords:
epigenetics;
vitamin C;
T helper cell;
DNA-pull down;
mass spectrometry;
ascorbate

Abbreviations used:
Cux1, cut like homeobox 1; CNS2, conserved non-coding sequence 2; Ehmt, euchromatic histone-lysine N-methyltransferase; PD-MS, DNA pull-down with subsequent mass spectrometric analysis; PD-WB, DNA pull-down with subsequent Western Blot analysis; Tcon, conventional T

cell; (i/n)Treg, (in vitro induced/natural) regulatory T cell; TSDR, Treg-specific demethylated region; vitC, vitamin C; Wiz, widely interspaced zinc finger motifs.

References

[1] E.M. Shevach, A.M. Thornton, tTregs, pTregs, and iTregs: similarities and differences, Immunol. Rev. 259 (2014) 88–102, https://doi.org/10.1007/s00401-007-0306-6.Huntington.

[2] J.D. Goldstein, L. Pérol, B. Zaragoza, A. Baeyens, G. Marodon, E. Piaggio, Role of cytokines in thymus- versus peripherally derived-regulatory T cell differentiation and function, Front. Immunol. 4 (2013) 1–10, https://doi.org/10.3389/fimmu.2013.00155.

[3] W. Chen, W. Jin, N. Hardegen, K.-J. Lei, L. Li, N. Marinos, G. McGrady, S.M. Wahl, Conversion of peripheral CD4+ CD25− naive T cells to CD4+CD25+ regulatory T cells by TGF-beta induction of transcription factor Foxp3, J. Exp. Med. 198 (2003) 1875–1886, https://doi.org/10.1084/jem.20030152.

[4] S. Floess, J. Freyer, C. Siewert, U. Baron, S. Olek, J. Polansky, K. Schlawe, H.D. Chang, T. Bopp, E. Schmitt, S. Klein-Hessling, E. Serfling, A. Hamann, J. Huehn, Epigenetic control of the foxp3 locus in regulatory T cells, PLoS Biol. 5 (2007) 169–178, https://doi.org/10.1371/journal.pbio.0050038.

[5] J.K. Polansky, K. Kretschmer, J. Freyer, S. Floess, A. Garbe, U. Baron, S. Olek, A. Hamann, H. von Boehmer, J. Huehn, DNA methylation controls Foxp3 gene expression, Eur. J. Immunol. 38 (2008) 1654–1663, https://doi.org/10.1002/eji.200838105.

[6] W. Fu, A. Ergun, T. Lu, J.A. Hill, S. Haxhinasto, M.S. Fassett, R. Gazit, S. Adoro, L. Glimcher, S. Chan, P. Kastner, D. Rossi, J.J. Collins, D. Mathis, C. Benoist, A multiply redundant genetic switch "locks in" the transcriptional signature of regulatory T cells, Nat. Immunol. 13 (2012) 972–980, https://doi.org/10.1038/ni.2420.

[7] Y. Kitagawa, N. Ohkura, Y. Kidani, A. Vandenbon, K. Hirota, R. Kawakami, K. Yasuda, D. Motooka, S. Nakamura, M. Kondo, I. Taniuchi, T. Kohwi-Shigematsu, S. Sakaguchi, Guidance of regulatory T cell development by Satb1-dependent super-enhancer establishment, Nat. Immunol. 18 (2016) 173–183, https://doi.org/10.1038/ni.3646.

[8] S. Hori, T. Nomura, S. Sakaguchi, Control of regulatory T cell development by the transcription factor Foxp3, Science. 299 (2003) 1057–1061, https://doi.org/10.1002/ajim.20072.

[9] J.D. Fontenot, M.A. Gavin, A.Y. Rudensky, Foxp3 programs the development and function of CD4+CD25+ regulatory T cells, Nat. Immunol. 4 (2003) 330–336, https://doi.org/10.1038/ni904.

[10] N. Ohkura, M. Hamaguchi, H. Morikawa, K. Sugimura, A. Tanaka, Y. Ito, M. Osaki, Y. Tanaka, R. Yamashita, N. Nakano, J. Huehn, H.J. Fehling, T. Sparwasser, K. Nakai, S. Sakaguchi, T cell receptor stimulation-induced epigenetic changes and Foxp3 expression are independent and complementary events required for Treg cell development, Immunity. 37 (2012) 785–799, https://doi.org/10.1016/j.immuni.2012.09.010.

[11] Y. Zheng, S. Josefowicz, A. Chaudhry, X.P. Peng, K. Forbush, A.Y. Rudensky, Role of conserved non-coding DNA elements in the Foxp3 gene in regulatory T-cell fate, Nature. 463 (2010) 808–812, https://doi.org/10.1038/Nature08750.

[12] D. Rudra, P. DeRoos, A. Chaudhry, R.E. Niec, A. Arvey, R.M. Samstein, C. Leslie, S.A. Shaffer, D.R. Goodlett, A.Y. Rudensky, Transcription factor Foxp3 and its protein partners form a complex regulatory network, Nat. Immunol. 13 (2012) 1010–1019, https://doi.org/10.1038/ni.2402.

[13] A. Toker, D. Engelbert, G. Garg, J.K. Polansky, S. Floess, T. Miyao, U. Baron, S. Düber, R. Geffers, P. Giehr, S. Schallenberg, K. Kretschmer, S. Olek, J. Walter, S. Weiss, S. Hori, A. Hamann, J. Huehn, Active demethylation of the Foxp3 locus leads to the generation of stable regulatory T cells within the thymus, J. Immunol. 190 (2013) 3180–3188, https://doi.org/10.4049/jimmunol.1203473.

[14] H.-P. Kim, W.J. Leonard, CREB/ATF-dependent T cell receptor-induced FoxP3 gene expression: a role for DNA methylation, J. Exp. Med. 204 (2007) 1543–1551, https://doi.org/10.1084/jem.20070109.

[15] J.K. Polansky, L. Schreiber, C. Thelemann, L. Ludwig, M. Krüger, R. Baumgrass, S. Cording, S. Floess, A. Hamann, J. Huehn, Methylation matters: binding of Ets-1 to the demethylated Foxp3 gene contributes to the stabilization of Foxp3 expression in regulatory T cells, J. Mol. Med. 88 (2010) 1029–1040, https://doi.org/10.1007/s00109-010-0642-1.

[16] C. Ogawa, Y. Tone, M. Tsuda, C. Peter, H. Waldmann, M. Tone, TGF-β-mediated Foxp3 gene expression is cooperatively regulated by Stat5, Creb, and AP-1 through CNS2, J. Immunol 192 (2014) 475–483, https://doi.org/10.4049/jimmunol.1301892.

[17] Y. Tone, K. Furuuchi, Y. Kojima, M.L. Tykocinski, M.I. Greene, M. Tone, Smad3 and NFAT cooperate to induce Foxp3 expression through its enhancer, Nat. Immunol. 9 (2008) 194–202, https://doi.org/10.1038/ni1549.

[18] S.M. Schlenner, B. Weigmann, Q. Ruan, Y. Chen, H. von Boehmer, Smad3 binding to the foxp3 enhancer is dispensable for the development of regulatory T cells with the exception of the gut, J. Exp. Med. 209 (2012) 1529–1535, https://doi.org/10.1084/jem.20112646.

[19] S.Z. Josefowicz, R.E. Niec, H.Y. Kim, P. Treuting, T. Chinen, Y. Zheng, D.T. Umetsu, A.Y. Rudensky, Extrathymically generated regulatory T cells control mucosal Th2 inflammation, Nature. 482 (2012) 395–399, https://doi.org/10.1038/nature10772.

[20] V.S. Nair, M.H. Song, M. Ko, K.I. Oh, DNA demethylation of the Foxp3 enhancer is maintained through modulation of ten–eleven-translocation and DNA methyltransferases, Mol. Cells 39 (2016) 888–897, https://doi.org/10.14348/molcells.2016.0276.

[21] V.S. Nair, K.I. Oh, Down-regulation of Tet2 prevents TSDR demethylation in IL2 deficient regulatory T cells, Biochem. Biophys. Res. Commun. 450 (2014) 918–924, https://doi.org/10.1016/j.bbrc.2014.06.110.

[22] X. Yue, S. Trifari, T. Äijö, A. Tsagaratou, W.A. Pastor, J.A. Zepeda-Martínez, C.-W.J. Lio, X. Li, Y. Huang, P. Vijayanand, H. Lähdesmäki, A. Rao, Control of Foxp3 stability through modulation of TET activity, J. Exp. Med. 213 (2016) 377–397, https://doi.org/10.1084/jem.20151438.

[23] Y. Feng, A. Arvey, T. Chinen, J. Van Der Veeken, G. Gasteiger, A.Y. Rudensky, Control of the inheritance of regulatory T cell identity by a cis element in the foxp3 locus, Cell. 158 (2014) 749–763, https://doi.org/10.1016/j.cell.2014.07.031.

[24] X. Li, Y. Liang, M. Leblanc, C. Benner, Y. Zheng, Function of a foxp3 cis-element in protecting regulatory T cell identity, Cell. 158 (2014) 734–748, https://doi.org/10.1016/j.cell.2014.07.030.

[25] V.S. Nair, M.H. Song, K.I. Oh, Vitamin C facilitates demethylation of the Foxp3 enhancer in a Tet-dependent manner, J. Immunol. 196 (2016) 2119–2131, https://doi.org/10.4049/jimmunol.1502352.

[26] E. Nikolouli, M. Hardtke-Wolenski, M. Hapke, M. Beckstette, R. Geffers, S. Floess, E. Jaeckel, J. Huehn, Alloantigen-induced regulatory T cells generated in presence of vitamin C display enhanced stability of Foxp3 expression and promote skin allograft acceptance, Front. Immunol. 8 (2017) 748, https://doi.org/10.3389/fimmu.2017.00748.

[27] M. Tachibana, K. Sugimoto, T. Fukushima, Y. Shinkai, Set domain-containing protein, G9a, is a novel lysine-preferring mammalian histone methyltransferase with hyperactivity and specific selectivity to lysines 9 and 27 of histone H3, J. Biol. Chem. 276 (2001) 25309–25317, https://doi.org/10.1074/jbc.M101914200.

[28] M. Tachibana, K. Sugimoto, M. Nozaki, J. Ueda, T. Ohta, M. Ohki, M. Fukuda, N. Takeda, H. Niida, H. Kato, Y. Shinkai, G9a histone methyltransferase plays a dominant role in euchromatic histone H3 lysine 9 methylation and is essential for early embryogenesis, Genes Dev. 16 (2002) 1779–1791, https://doi.org/10.1101/gad.989402.

[29] J.C. Rice, S.D. Briggs, B. Ueberheide, C.M. Barber, J. Shabanowitz, D.F. Hunt, Y. Shinkai, C.D. Allis, Histone methyltransferases direct different degrees of methylation to define distinct chromatin domains, Mol. Cell 12 (2003) 1591–1598, https://doi.org/10.1016/S1097-2765(03)00479-9.

[30] M. Tachibana, J. Ueda, M. Fukuda, N. Takeda, T. Ohta, H. Iwanari, T. Sakihama, T. Kodama, T. Hamakubo, Y. Shinkai, Histone methyltransferases G9a and GLP form heteromeric complexes and are both crucial for methylation of euchromatin at H3-K9, Genes Dev. 19 (2005) 815–826, https://doi.org/10.1101/gad.1284005.

[31] D.C. Leung, K.B. Dong, I.A. Maksakova, P. Goyal, R. Appanah, S. Lee, M. Tachibana, Y. Shinkai, B. Lehnertz, D.L. Mager, F. Rossi, M.C. Lorincz, Lysine methyltransferase G9a is required for de novo DNA methylation and the establishment, but not the maintenance, of proviral silencing, Proc. Natl. Acad. Sci. U. S. A 108 (2011) 5718–5723, https://doi.org/10.1073/pnas.1014660108.

[32] A. Fiszbein, L.E. Giono, A. Quaglino, B.G. Berardino, L. Sigaut, C. von Bilderling, I.E. Schor, J.H.E. Steinberg, M. Rossi, L.I. Pietrasanta, J.J. Caramelo, A. Srebrow, A.R. Kornblihtt, Alternative splicing of G9a regulates neuronal differentiation, Cell Rep. 14 (2016) 2797–2808, https://doi.org/10.1016/j.celrep.2016.02.063.

[33] K. Skourti-Stathaki, K. Kamieniarz-Gdula, N.J. Proudfoot, R-loops induce repressive chromatin marks over mammalian gene terminators, Nature. 516 (2014) 436–439, https://doi.org/10.1038/nature13787.

[34] B. Wen, H. Wu, Y. Shinkai, R.A. Irizarry, A.P. Feinberg, Large histone H3 lysine 9 dimethylated chromatin blocks distinguish differentiated from embryonic stem cells, Nat. Genet. 41 (2009) 246–250, https://doi.org/10.1038/ng.297.

[35] N. Feldman, A. Gerson, J. Fang, E. Li, Y. Zhang, Y. Shinkai, H. Cedar, Y. Bergman, G9a-mediated irreversible epigenetic inactivation of Oct-3/4 during early embryogenesis, Nat. Cell Biol. 8 (2006) 188–194, https://doi.org/10.1038/ncb1353.

[36] S. Epsztejn-Litman, N. Feldman, M. Abu-Remaileh, Y. Shufaro, A. Gerson, J. Ueda, R. Deplus, F. Fuks, Y. Shinkai, H. Cedar, Y. Bergman, De novo DNA methylation promoted by G9a prevents reprogramming of embryonically silenced genes, Nat. Struct. Mol. Biol. 15 (2008) 1176–1183, https://doi.org/10.1038/nsmb.1476.

[37] P.O. Estève, G.C. Hang, A. Smallwood, G.R. Feehery, O. Gangisetty, A.R. Karpf, M.F. Carey, S. Pradhan, Direct interaction between DNMT1 and G9a coordinates DNA and histone methylation during replication, Genes Dev. 20 (2006) 3089–3103, https://doi.org/10.1101/gad.1463706.

[38] Y. Chang, L. Sun, K. Kokura, J.R. Horton, M. Fukuda, A. Espejo, V. Izumi, J.M. Koomen, M.T. Bedford, X. Zhang, Y. Shinkai, J. Fang, X. Cheng, MPP8 mediates the interactions between DNA methyltransferase Dnmt3a and H3K9 methyltransferase GLP/G9a, Nat. Commun. 2 (2011) 533, https://doi.org/10.1038/ncomms1549.

[39] K.B. Dong, I.A. Maksakova, F. Mohn, D. Leung, R. Appanah, S. Lee, H.W. Yang, L.L. Lam, D.L. Mager, D. Schübeler, M. Tachibana, Y. Shinkai, M.C. Lorincz, D. Schübeler, M. Tachibana, Y. Shinkai, M.C. Lorincz, DNA methylation in ES cells requires the lysine methyltransferase G9a but not its catalytic activity, EMBO J 27 (2008) 2691–2701, https://doi.org/10.1038/emboj.2008.193.

[40] M. Tachibana, Y. Matsumura, M. Fukuda, H. Kimura, Y. Shinkai, G9a/GLP complexes independently mediate H3K9 and DNA methylation to silence transcription, EMBO J. 27 (2008) 2681–2690, https://doi.org/10.1038/emboj.2008.192.

[41] K. Ikegami, M. Iwatani, M. Suzuki, M. Tachibana, Y. Shinkai, S. Tanaka, J.M. Greally, S. Yagi, N. Hattori, K. Shiota, Genome-wide and locus-specific DNA hypomethylation in G9a deficient mouse embryonic stem cells, Genes Cells 12 (2007) 1–11, https://doi.org/10.1111/j.1365-2443.2006.01029.x.

[42] G. Auclair, J. Borgel, L.A. Sanz, J. Vallet, S. Guibert, M. Dumas, P. Cavelier, M. Girardot, T. Forné, R. Feil, M. Weber, EHMT2 directs DNA methylation for efficient gene silencing in mouse embryos, Genome Res. 26 (2015) 1–11, https://doi.org/10.1101/gr.198291.115.

[43] G. Mittler, F. Butter, M. Mann, A SILAC-based DNA protein interaction screen that identifies candidate binding proteins to functional DNA elements, Genome Res 19 (2009) 284–293, https://doi.org/10.1101/gr.081711.108.

[44] S.-E. Ong, B. Blagoev, I. Kratchmarova, D.B. Kristensen, H. Steen, A. Pandey, M. Mann, Stable isotope labeling by amino acids in cell culture, SILAC, as a simple and accurate approach to expression proteomics, Mol. Cell. Proteomics 1 (2002) 376–386, https://doi.org/10.1074/mcp.M200025-MCP200.

[45] Y. Okada, H. Nobori, M. Shimizu, M. Watanabe, M. Yonekura, T. Nakai, Y. Kamikawa, A. Wakimura, N. Funahashi, H. Naruse, A. Watanabe, D. Yamasaki, S.I. Fukada, K. Yasui, K. Matsumoto, T. Sato, K. Kitajima, T. Nakano, W.C. Aird, T. Doi, Multiple ETS family proteins regulate PF4 gene expression by binding to the same ETS binding site, PLoS One 6 (2011), e24837, https://doi.org/10.1371/journal.-pone.0024837.

[46] Z. Xin, M. Tachibana, M. Guggiari, E. Heard, Y. Shinkai, J. Wagstaff, Role of histone methyltransferase G9a in CpG methylation of the Prader–Willi syndrome imprinting center, J. Biol. Chem. 278 (2003) 14996–15000, https://doi.org/10.1074/jbc.M211753200.

[47] K. Myant, A. Termanis, A.Y.M. Sundaram, T. Boe, C. Li, C. Merusi, J. Burrage, J.I. De Las Heras, I. Stancheva, LSH and G9a/GLP complex are required for developmentally programmed DNA methylation, Genome Res. 21 (2011) 83–94, https://doi.org/10.1101/gr.108498.110.

[48] T. Zhang, A. Termanis, B. Özkan, X.X. Bao, J. Culley, F. de Lima Alves, J. Rappsilber, B. Ramsahoye, I. Stancheva, G9a/GLP complex maintains imprinted DNA methylation in

embryonic stem cells, Cell Rep. 15 (2016) 77–85, https://doi.org/10.1016/j.celrep.2016.03.007.
[49] M. Vedadi, D. Barsyte-lovejoy, F. Liu, S. Rival-Gervier, A. Allali-hassani, V. Labrie, T.J. Wigle, P.A. Dimaggio, A. Gregory, A. Siarheyeva, A. Dong, W. Tempel, S. Wang, I. Chau, T.J. Mangano, X. Huang, C.D. Simpson, S.G. Pattenden, J.L. Norris, D.B. Kireev, A. Tripathy, B.L. Roth, W.P. Janzen, B.A. Garcia, A. Petronis, J. Ellis, P.J. Brown, S.V. Frye, C.H. Arrowsmith, J. Jin, A chemical probe selectively inhibits G9a and GLP methyltransferase activity in cells, Nat Chem Biol 7 (2012) 566–574, https://doi.org/10.1038/nchembio.599.A.
[50] Y. Chang, T. Ganesh, J.R. Horton, A. Spannhoff, J. Liu, A. Sun, X. Zhang, M.T. Bedford, Y. Shinkai, J.P. Snyder, X. Cheng, Adding a lysine mimic in the design of potent inhibitors of histone lysine methyltransferases, J. Mol. Biol. 400 (2010) 1–7, https://doi.org/10.1016/j.jmb.2010.04.048.
[51] Y. Tsukada, J. Fang, H. Erdjument-Bromage, M.E. Warren, C.H. Borchers, P. Tempst, Y. Zhang, Histone demethylation by a family of JmjC domain-containing proteins, Nature. 439 (2006) 811–816, https://doi.org/10.1038/nature04433.
[52] J.I. Young, S. Züchner, G. Wang, Regulation of the epigenome by vitamin C, Annu. Rev. Nutr. 35 (2015) 545–564, https://doi.org/10.1146/annurev-nutr-071714-034228.
[53] S. Hamada, T.D. Kim, T. Suzuki, Y. Itoh, H. Tsumoto, H. Nakagawa, R. Janknecht, N. Miyata, Synthesis and activity of N-oxalylglycine and its derivatives as Jumonji C-domain-containing histone lysine demethylase inhibitors, Bioorg. Med. Chem. Lett. 19 (2009) 2852–2855, https://doi.org/10.1016/j.bmcl.2009.03.098.
[54] R. Amouroux, B. Nashun, K. Shirane, S. Nakagawa, P.W.S. Hill, Z. D'Souza, M. Nakayama, M. Matsuda, A. Turp, E. Ndjetehe, V. Encheva, N.R. Kudo, H. Koseki, H. Sasaki, P. Hajkova, De novo DNA methylation drives 5hmC accumulation in mouse zygotes, Nat. Cell Biol. 18 (2016) 225–233, https://doi.org/10.1038/ncb3296.
[55] H.G. Roider, A. Kanhere, T. Manke, M. Vingron, Predicting transcription factor affinities to DNA from a biophysical model, Bioinformatics. 23 (2007) 134–141, https://doi.org/10.1093/bioinformatics/btl565.
[56] H. Nishio, M.J. Walsh, CCAAT displacement protein/cut homolog recruits G9a histone lysine methyltransferase to repress transcription, Proc. Natl. Acad. Sci. U. S. A. 101 (2004) 11257–11262, https://doi.org/10.1073/pnas.0401343101.
[57] J. Ueda, M. Tachibana, T. Ikura, Y. Shinkai, Zinc finger protein wiz links G9a/GLP histone methyltransferases to the co-repressor molecule CtBP, J. Biol. Chem. 281 (2006) 20120–20128, https://doi.org/10.1074/jbc.M603087200.
[58] C.-P. Chaturvedi, B. Somasundaram, K. Singh, R.L. Carpenedo, W.L. Stanford, F.J. Dilworth, M. Brand, Maintenance of gene silencing by the coordinate action of the H3K9 methyltransferase G9a/KMT1C and the H3K4 demethylase Jarid1a/KDM5A, Proc. Natl. Acad. Sci. U. S. A. 109 (2012) 18845–18850, https://doi.org/10.1073/pnas.1213951109.
[59] C. Bian, Q. Chen, X. Yu, The zinc finger proteins ZNF644 and WIZ regulate the G9A/GLP complex for gene repression, Elife. 2015 (2015), e05606, https://doi.org/10.7554/eLife.05606.
[60] L. Isbel, L. Prokopuk, H. Wu, L. Daxinger, H. Oey, A. Spurling, A.J. Lawther, M.W. Hale, E. Whitelaw, Wiz binds active promoters and CTCF-binding sites and is required for normal behaviour in the mouse, Elife. 5 (2016), e15082, https://doi.org/10.7554/eLife.15082.
[61] P. Michl, A.R. Ramjaun, O.E. Pardo, P.H. Warne, M. Wagner, R. Poulsom, C. D'Arrigo, K. Ryder, A. Menke, T. Gress, J. Downward, CUTL1 is a target of TGF-beta signaling that enhances cancer cell motility and invasiveness, Cancer Cell 7 (2005) 521–532, https://doi.org/10.1016/j.ccr.2005.05.018.
[62] F. Antignano, C. Zaph, Regulation of CD4+ T-cell differentiation and inflammation by repressive histone methylation, Immunol. Cell Biol. 93 (2015) 245–252, https://doi.org/10.1038/icb.2014.115.
[63] L.R. Thomas, H. Miyashita, R.M. Cobb, S. Pierce, M. Tachibana, E. Hobeika, M. Reth, Y. Shinkai, E.M. Oltz, Functional analysis of histone methyltransferase G9a in B and T lymphocytes, J. Immunol. 181 (2008) 485–493, https://doi.org/10.4049/jimmunol.181.1.485.
[64] B. Lehnertz, J.P. Northrop, F. Antignano, K. Burrows, S. Hadidi, S.C. Mullaly, F.M.V. Rossi, C. Zaph, Activating and inhibitory functions for the histone lysine methyltransferase G9a in T helper cell differentiation and function, J. Exp. Med 207 (2010) 915–922, https://doi.org/10.1084/jem.20100363.
[65] F. Antignano, K. Burrows, M.R. Hughes, J.M. Han, K.J. Kron, N.M. Penrod, M.J. Oudhoff, S.K.H. Wang, P.H. Min, M.J. Gold, A.L. Chenery, M.J.S. Braam, T.C. Fung, F.M.V. Rossi, K.M. McNagny, C.H. Arrowsmith, M. Lupien, M.K. Levings, C. Zaph, Methyltransferase G9A regulates T cell differentiation during murine intestinal inflammation, J. Clin. Invest 124 (2014) 1945–1955, https://doi.org/10.1172/JCI69592.
[66] A. Schaefer, S.C. Sampath, A. Intrator, A. Min, T.S. Gertler, D.J. Surmeier, A. Tarakhovsky, P. Greengard, Control of cognition and adaptive behavior by the GLP/G9a epigenetic suppressor complex, Neuron. 64 (2009) 678–691, https://doi.org/10.1016/j.neuron.2009.11.019.
[67] V. Battisti, J. Pontis, E. Boyarchuk, L. Fritsch, P. Robin, S. Ait-Si-Ali, V. Joliot, Unexpected distinct roles of the related histone H3 lysine 9 methyltransferases G9a and G9a-like protein in myoblasts, J. Mol. Biol. 428 (2016) 2329–2343, https://doi.org/10.1016/j.jmb.2016.03.029.
[68] D.J. Verbaro, N. Sakurai, B. Kim, Y. Shinkai, T. Egawa, Cutting edge: the histone methyltransferase G9a is required for silencing of helper T lineage-associated genes in proliferating CD8 T cells, J. Immunol. 200 (2018) 3891–3896, https://doi.org/10.4049/jimmunol.1701700.
[69] W. Luo, D.G. Skalnik, CCAAT displacement protein competes with multiple transcriptional activators for binding to four sites in the proximal gp91phox promoter, J. Biol. Chem. 271 (1996) 18203–18210, https://doi.org/10.1074/JBC.271.30.18203.
[70] F. Mailly, G. Bérubé, R. Harada, P.L. Mao, S. Phillips, A. Nepveu, The human cut homeodomain protein can repress gene expression by two distinct mechanisms: active repression and competition for binding site occupancy, Mol. Cell. Biol. 16 (1996) 5346–5357, https://doi.org/10.1128/MCB.16.10.5346.
[71] E.C. Kim, J.S. Lau, S. Rawlings, A.S. Lee, Positive and negative regulation of the human thymidine kinase promoter mediated by CCAAT binding transcription factors NF-Y/CBF, dbpA, and CDP/cut., Cell Growth Differ. 8 (1997) 1329–1338. doi:10.1.1.578.1173.
[72] G. Marziali, E. Perrotti, R. Ilari, E.M. Coccia, R. Mantovani, U. Testa, A. Battistini, The activity of the CCAAT-box binding factor NF-Y is modulated through the regulated expression of its A subunit during monocyte to macrophage differentiation: regulation of tissue-specific genes through a ubiquitous transcription factor, Blood. 93 (1999) 519–526.

[73] R. Mantovani, The molecular biology of the CCAAT-binding factor NF-Y, Gene. 239 (1999) 15–27, https://doi.org/10.1016/S0378-1119(99)00368-6.
[74] M.H. Song, V.S. Nair, K.I. Oh, Vitamin C enhances the expression of IL17 in a Jmjd2-dependent manner, BMB Rep. 50 (2017) 49–54, https://doi.org/10.5483/BMBRep.2017.50.1.193.
[75] E. Flashman, S.L. Davies, K.K. Yeoh, C.J. Schofield, Investigating the dependence of the hypoxia-inducible factor hydroxylases (factor inhibiting HIF and prolyl hydroxylase domain 2) on ascorbate and other reducing agents, Biochem. J. 427 (2010) 135–142, https://doi.org/10.1042/BJ20091609.
[76] C. Kuiper, G.U. Dachs, M.J. Currie, M.C.M. Vissers, Intracellular ascorbate enhances hypoxia-inducible factor (HIF)-hydroxylase activity and preferentially suppresses the HIF-1 transcriptional response, Free Radic. Biol. Med. 69 (2014) 308–317, https://doi.org/10.1016/j.freeradbiomed.2014.01.033.
[77] A. Ang, J.M. Pullar, M.J. Currie, M.C.M. Vissers, Vitamin C and immune cell function in inflammation and cancer, Biochem. Soc. Trans. 46 (2018) 1147–1159, https://doi.org/10.1042/bst20180169.
[78] D. Haribhai, W. Lin, L.M. Relland, N. Truong, C.B. Williams, T.A. Chatila, Regulatory T cells dynamically control the primary immune response to foreign antigen, J. Immunol. 178 (2007) 2961–2972, https://doi.org/10.4049/jimmunol.178.5.2961.
[79] U.K. Laemmli, Cleavage of structural proteins during the assembly of the head of bacteriophage T4, Nature. 227 (1970) 680–685, https://doi.org/10.1038/227680a0.
[80] S. Frischbutter, C. Gabriel, H. Bendfeldt, A. Radbruch, R. Baumgrass, Dephosphorylation of Bcl-10 by calcineurin is essential for canonical NF-kB activation in Th cells, Eur. J. Immunol. 41 (2011) 2349–2357, https://doi.org/10.1002/eji.201041052.
[81] S.C. Bendall, C. Hughes, M.H. Stewart, B. Doble, M. Bhatia, G.A. Lajoie, Prevention of amino acid conversion in SILAC experiments with embryonic stem cells, Mol. Cell. Proteomics 7 (2008) 1587–1597, https://doi.org/10.1074/mcp.M800113-MCP200.
[82] M. Marcilla, A. Alpizar, A. Paradela, J.P. Albar, A systematic approach to assess amino acid conversions in SILAC experiments, Talanta. 84 (2011) 430–436, https://doi.org/10.1016/j.talanta.2011.01.050.
[83] F.A. Ran, P.D. Hsu, J. Wright, V. Agarwala, D.A. Scott, F. Zhang, Genome engineering using the CRISPR–Cas9 system, Nat. Protoc. 8 (2013) 2281–2308, https://doi.org/10.1038/nprot.2013.143.